

**DIVISION OF COAL AND ENERGY TECHNOLOGY**  
Institute of Minerals, Energy and Construction

**INVESTIGATION REPORT CET/IR238**

**TRAFFIC GENERATED POLLUTION NEAR  
ROADS AND HIGHWAYS : MODELS AND  
MEASUREMENTS**

by

**D.J. Williams, J.N. Carras, Deloor Shenouda,  
M.S. Drummond and A.L. Lange**

**Final Report Prepared for  
RTA**

**North Ryde Laboratory  
P.O. Box 136, North Ryde  
NSW 2113**

**March, 1994**



## TABLE OF CONTENTS

	Page
Summary	1
1 INTRODUCTION	2
2 EXPERIMENTAL METHODS	2
3 RESULTS AND DISCUSSION	5
3.1 Modelling Pollution from Roadways	5
3.2 Modelling Motor Vehicle Emissions	5
3.2.1 Power-based Exhaust Emission Model	7
3.2.2 Validation of Exhaust Emission Model	12
3.2.2.1 Spark Ignition Vehicles	12
3.2.2.2 Compression Ignition(diesel) Vehicles	20
3.3 Dispersion Modelling	28
3.3.1 CHOCK	32
3.3.2 HIWAY-2	33
3.3.3 CALINE-4	34
3.4 Model Performance	35
4 RECOMMENDATIONS AND CONCLUSIONS	62
5 REFERENCES	63

### LIST OF TABLES

Table 1.	Comparison of predicted and measured exhaust emissions for pre-1986 and post 1985 cars.
Table 2.	Data Summary - 5 March 1992 - Epping Hwy
Table 3.	Data Summary - 5 May 1992 - Epping Hwy
Table 4.	Data Summary - 6 May 1992 - Epping Hwy
Table 5.	Data Summary - 26 May 1992 - James Ruse Drive
Table 6.	Data Summary - 16 June 1992 - James Ruse Drive
Table 7.	Data Summary - 13 Jan 1993 - Epping Hwy
Table 8.	Data Summary - 6 April 1993 - Homebush
Table 9.	Deterioration factors for SI vehicles
Table 10.	Examples of typical average vehicle emission rates

## LIST OF FIGURES

- Figure 1. Schematic showing method of deploying CSIRO instrumented vehicle alongside an arterial road.
- Figure 2. Comparison of predicted and measured ADR37 fuel economy for pre-1986 and post-1985 SI vehicles.
- Figure 3. Comparison of predicted and measured ADR37 CO emissions for pre-1986 SI vehicles .
- Figure 4. Comparison of predicted and measured ADR37 HC emissions for pre-1986 SI vehicles.
- Figure 5. Comparison of predicted and measured ADR37 NO<sub>x</sub> emissions for pre-1986 SI vehicles..
- Figure 6. Comparison of predicted and measured ADR37 CO emissions for post-1985 SI vehicles.
- Figure 7. Comparison of predicted and measured ADR37 HC emissions for post-1985 SI vehicles.
- Figure 8. Comparison of predicted and measured ADR37 NO<sub>x</sub> emissions for post-1985 SI vehicles.
- Figure 9. ADR27 drive cycle and it's division into freeway (F), arterial (A) and congested (C) segments.
- Figure 10. Comparison of predicted and measured ADR37 fuel economy for light-duty diesels.
- Figure 11. Comparison of predicted and measured ADR37 CO emissions for light-duty diesels.
- Figure 12. Comparison of predicted and measured ADR37 HC emissions for light-duty diesels.
- Figure 13. Comparison of predicted and measured ADR37 NO<sub>x</sub> emissions for light-duty diesels.
- Figure 14. Comparison of predicted CO emission rate for 2.5 L unleaded SI vehicle with US EMFAC predictions as a function of speed.
- Figure 15. Comparison of predicted HC emission rate for 2.5 L unleaded SI vehicle with US EMFAC predictions as a function of speed.

Figure 16. Comparison of predicted  $\text{NO}_x$  emission rate for 2.5 L unleaded SI vehicle with US EMFAC predictions as a function of speed.

Figure 17. Effect of slope on power fuel consumption as a function of speed for 2.5L SI vehicle

Figure 18. Predicted v measured  $\text{CO}_2$  concentration for HIWAY and CALINE : slope =  $0^\circ$ .

Figure 19. Predicted v measured  $\text{CO}_2$  concentration for HIWAY and CALINE : slope =  $0.5^\circ$ .

Figure 20. Predicted v measured  $\text{CO}_2$  concentration for HIWAY and CALINE : slope =  $1.0^\circ$ .

Figure 21. Predicted v measured  $\text{CO}_2$  concentration for HIWAY and CALINE : slope =  $1.5^\circ$ .

Figure 22. Predicted v measured  $\text{CO}_2$  concentration for HIWAY and CHOCK: slope =  $1.0^\circ$ .

Figure 23. Predicted v measured  $\text{CO}_2$  concentration for HIWAY and CALINE : slope =  $0.5^\circ$ . sampling ht = 2.5m, distance = 30 m from roadside.

Figure 24. Comparison of predicted  $\text{CO}_2$  concentrations from HIWAY, CALINE and CALINE-\* (slope= $0^\circ$ ) with measured values as a function of wind speed: distance = 30 m from roadside.

Figure 25. Comparison of predicted  $\text{CO}_2$  concentrations from HIWAY, CALINE and CALINE-\* (slope= $0.5^\circ$ ) with measured values as a function of wind speed: distance = 30 m from roadside.

Figure 26. Comparison of predicted  $\text{CO}_2$  concentrations from HIWAY, CALINE and CALINE-\* (slope= $1.0^\circ$ ) with measured values as a function of wind speed: distance = 30 m from roadside.

Figure 27. Comparison of predicted  $\text{CO}_2$  concentrations from HIWAY, CALINE and CALINE-\* (slope= $1.5^\circ$ ) with measured values as a function of wind speed: distance = 30 m from roadside.

Figure 28. Predicted v measured CO<sub>2</sub> concentration for HIWAY  
CALINE and CALINE-\* : slope = 1.0<sup>0</sup>.  
distance = 60 m from roadside.

Figure 29. Predicted v measured CO<sub>2</sub> concentration for HIWAY and  
CALINE-\* : slope = 1.0<sup>0</sup>.

Figure 30. Predicted v measured CO concentration for HIWAY and  
CALINE-\* : slope = 1.0<sup>0</sup>.

Figure 31. Predicted v measured HC concentration for HIWAY and  
CALINE-\* : slope = 1.0<sup>0</sup>.

Figure 32. Predicted v measured NO<sub>x</sub> concentration for HIWAY and  
CALINE-\* : slope = 1.0<sup>0</sup>.

## Summary

Emissions of carbon dioxide (CO<sub>2</sub>), carbon monoxide (CO), hydrocarbons (HC) and nitrogen oxides (NO<sub>x</sub>) from vehicles have been modelled by considering the instantaneous power requirements and using the expressions developed by Post et al, (1981). The emissions from both spark ignition (SI) and diesel vehicles have been included.

The model was used estimate fuel consumption and emissions over a standard driving cycle. When used for SI vehicles over a drive cycle, the influence of cold starts was quantified and allowance made, in the case of catalyst equipped vehicles, for catalyst warm-up and for variations in catalyst efficiency.

The model was validated against fuel consumption and emissions data obtained using ADR27 and ADR37 tests and against detailed, high time resolution analysis of ADR27 tests carried out by the Victorian EPA.

The emissions model was then used in conjunction with three pollution dispersion models viz: CHOCK (alias GM), HIWAY, CALINE and a slightly modified version of CALINE (CALINE-\*) to compare predicted concentrations with an experimental data-set. The data-set consisted of measurements of the pollutants CO<sub>2</sub>, CO, HC and NO<sub>x</sub> and were made under a variety of traffic and meteorological conditions. The measurements were made at locations up to 60m downwind from the roadside and to heights of 10m above the ground. A video camera was used to record the traffic flow, speed and type (classified simply as domestic, light or heavy commercial).

It has been demonstrated that this approach can provide good estimates of pollutant concentrations from suburban arterial roads, particularly when used with the last three dispersion models. Because of Sydney's hilly terrain, this method provides a more realistic and flexible approach to estimating vehicle pollution impacts in the metropolitan area.

## 1. INTRODUCTION

The CSIRO Division of Coal and Energy Technology in collaboration with the Roads and Traffic Authority of NSW has carried out a major study of the pollution generated near arterial roads by motor vehicles. The objectives of the study were:

- (1) To determine the concentrations of airborne pollutants generated by motor vehicles on arterial roads for a range of traffic conditions.
- (2) To relate these measurements to the flow and type of traffic and to the meteorology prevailing at the times of measurement.
- (3) To organise the data for input into existing air pollution models and evaluate their performance.

This report provides a detailed description of the vehicle emissions module and an evaluation of its performance with respect to emissions data produced by drive cycle testing. The module is used, in conjunction with dispersion models and field measurements of roadway pollution to predict pollutant concentrations near arterial roads.

## 2. EXPERIMENTAL METHODS

The experimental methodology employed to quantify traffic generated pollution has been described in an interim report (Williams et al., 1993). Briefly, it consisted of an instrumented vehicle equipped for measuring the gaseous pollutants carbon monoxide (CO), non-methane hydrocarbons (HC) and nitrogen oxides (NO<sub>x</sub>) as well as fine visibility-degrading particles as measured by a nephelometer. In addition, as carbon dioxide (CO<sub>2</sub>) produced by traffic is directly related to fuel consumption rate, this

species was also measured. Two simultaneous sampling positions were used. One was situated at the research vehicle, which was normally located about 30 m from the road under study, either in a side street or on a vacant lot. A large flexible sample line was then used to position the second sampling point within  $\pm 30$  m of the research vehicle. This allowed concentrations to be measured up to 60 m from the edge of a road. Both sample lines could also be deployed up to 10 m above the ground to assess the vertical extent of the pollution. Figure 1 shows a schematic of the overall method employed.

Meteorological data came from two Gill u.v.w. anemometers. These instruments provided the mean wind speed and direction as well as turbulence statistics at two heights. The lower height was fixed at 2.5 m, whilst the upper one was variable up to 10 m.

The data obtained from the instruments were recorded on chart and logged every second on a computer. Due to the number of inputs and the logging rate each hour of experiment resulted in about 1 M byte of data.

A video camera was also located strategically to record the traffic flow in both directions. The video-taped information was subsequently analysed to provide data on vehicle flow and type.

Data from each instrument were used to construct 2 to 30 minute averages of the CO<sub>2</sub>, CO, HC, and NO<sub>x</sub> concentrations as well as wind speed and direction.

The video data were examined and a manual count made of the vehicle flow, in both directions. The vehicles were classified by their appearance as domestic, light commercial or heavy commercial.



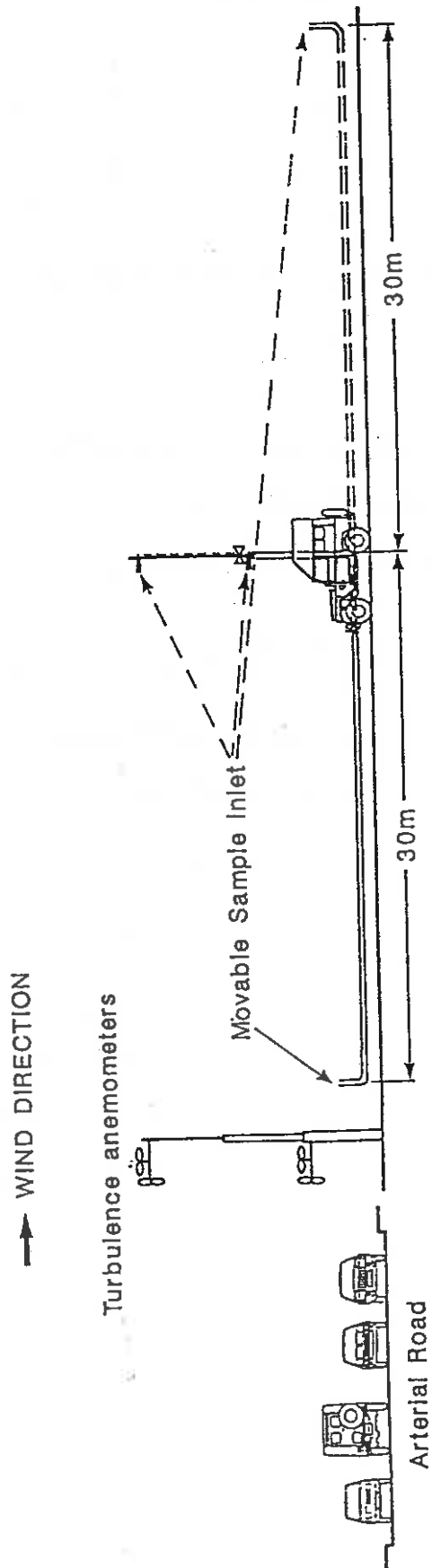


Figure 1. Schematic showing method of deploying CSIRO instrumented vehicle alongside an arterial road

### 3 RESULTS AND DISCUSSION

#### 3.1 Modelling Pollutants From Roadways

As noted in the previous report, there are three components to modelling the concentrations of traffic generated pollution near arterial roads. These are stated again here:

- (a) estimation of pollution source strength. This is a function of, *inter alia*, traffic speed, density and flow, vehicle type and road gradient.
- (b) simulation of the road link, including the number and width of the lanes, width of the median strip, road gradient and orientation.
- (c) modelling the dispersion of the pollution, which is a function of, *inter alia*, wind speed and direction, atmospheric stability, vehicle wake turbulence and local terrain.

#### 3.2 Modelling Motor Vehicle Emissions

One commonly-used approach is to take emissions data produced by subjecting vehicles to a standard drive cycle and adjust them to match the highway speed by means of a speed correction factor (SCF). This approach is used, for example, by the USEPA and the South Coast Air Resources Board, the latter body having developed the EMFAC7 methodology. EMFAC7 (the discussion here includes its component models E7WT and BURDEN7F) develops emission factors for both exhaust and evaporative emissions for different vehicle technology groups and weights them according to vehicle population and annual distance travelled. The model uses emission data from the Federal Test Procedure (FTP), an urban drive cycle used in the Australian ADR27 and ADR37 test procedures. Emissions from cold and hot starts are taken into account as well as stabilised running. These data are then adjusted for use in a given situation by four correction factors viz a mode correction

factor (BCF), a speed correction factor (SCF), a temperature correction factor (TCF), and a fuel correction factor (FCF). A fifth "miscellaneous" correction factor is also available if necessary. The various correction factors, particularly the BCF and SCF are specified for a given model year to take vehicle deterioration into account. The vehicle technology groups are identified as light duty automobiles, light, medium and heavy duty trucks, urban diesel buses, and motorcycles. These vehicles are then classified as catalyst or non-catalyst equipped gasoline fuelled vehicles or diesels.

Another, interesting, approach has been developed by the Victorian EPA (Carnovale et al., 1991). In this procedure, the ADR27 test cycle was split into segments representing three driving modes, viz freeway, arterial and congested roads, and the exhaust emissions from over 1500 vehicles, from different technology classes, were analysed on this split mode basis. Deterioration factors (g/km) were developed for CO, HC and NO<sub>x</sub> emissions for each 10,000 km travelled.

A limitation of methodologies such as EMFAC7 and that developed by the Victorian EPA is that they are more suitable to estimating emissions for an airshed or over a number of links rather than at a specific location. This is because airshed or multi-link modelling involves a range of driving conditions better approximated by the FTP related data. The limitation is particularly evident when attempting to model pollution near significant inclines.

However, even with this reservation to one side, it has been established that, despite the effort and detail that has gone into the US models, they do not, currently, provide reliable estimates of on-road pollutant emissions (Cadle et al., 1991). Analysis of air quality in well defined situations such as road tunnels shows that CO and HC concentrations are about twice those anticipated from the traffic type and density (Robinson et al., 1993), although NO<sub>x</sub> levels are only 50% higher. Guensler et al., 1993) measured the emissions from over 500 vehicles using 5 drive cycles with different average speeds. Whilst the average trend of the emissions over the different

average speed cycles conformed with that predicted by applying SCF to FTP data, the scatter was such that, at the 95% confidence level, they were unable to predict whether increasing the average speed of any particular trip would decrease or increase pollutant emissions. Although the reasons why actual emissions are so much higher than predicted are unclear, one of the factors undoubtedly concerns so-called open loop operation of catalyst equipped vehicles when uncontrolled exhaust emissions occur to avoid overheating the catalyst.

For our particular type of experimental database, which has data relating to fuel consumption, we have adopted what we believe to be a more realistic procedure based on the work of Kent et al., (1981). In this approach, the total instantaneous power required to propel the vehicle along the road is taken as the basis for estimating the fuel consumption and emission rates at that instant. The model, must of course, be capable of simulating drive cycle emissions and its performance when tested against emission data obtained from FTP cycle testing and the use of SCF is presented later.

### 3.2. 1 Power-Based Exhaust Emissions Model

The instantaneous power,  $Z_t$ , to propel a vehicle along is given by

$$Z_t = Z_d + Z_r + Z_a + Z_e \quad (1)$$

where  $Z_d$  is the power required to overcome the vehicle drive-train resistance,  $Z_r$  the tyre rolling resistance,  $Z_a$  the aerodynamic drag and  $Z_e$  the inertial and gravitational resistance.

According to Richardson (1982) the contributing terms are given by

$$Z_d = 2.36 \times 10^{-7} v^2 M \quad (2)$$

where  $M$  is in kilograms,  $v$  is the vehicle speed in km/hr and  $Z_d$  is in kW.

$$Z_r = (3.72 \times 10^{-5} v + 3.09 \times 10^{-8} v^2) M \quad (3)$$

$$Z_a = 1.29 \times 10^{-5} C_d A v^3 \quad (4)$$

where  $C_d$  is the aerodynamic drag coefficient and  $A$  is the frontal area of the vehicle ( $m^2$ ).

$$Z_e = (ma + mg \sin \theta)v \quad (5)$$

where  $a$  is the vehicle acceleration,  $v$  is the vehicle speed,  $g$  is the acceleration due to gravity and  $\theta$  the gradient.

The fuel consumption rate,  $F_c$ , is related to the total instantaneous power of the vehicle by the linear relation

$$F_c = \alpha + \beta Z_t \quad (6)$$

where the value of  $\alpha$  is the fuel consumption rate at idle conditions in ml/min and  $\beta$  is the measure of the efficiency of power generation (in ml/min kW). For spark ignition vehicles, Post et al., (1981) found that the idle fuel flow rate was a function of engine capacity, EC, such that

$$\alpha = 9.9 \text{ EC} \quad (7)$$

These workers tested their formulations by comparing the total fuel consumption over a standard driving cycle with the values computed from equation (6) above for over 100 vehicles and found good correlations between fuel consumption and power demand. They also found that  $\alpha$  and  $\beta$  for a given vehicle would vary with the state of tune and vehicle condition.

The problem now is to develop formulations for estimating exhaust emissions. For spark ignition engines, CO is thought to result largely from thermal equilibrium in the combustion process frozen as the temperature drops rapidly from 2500-3000K during the expansion part of the cycle (see eg Flagan and Seinfeld, 1988). The actual proportion of the fuel carbon that ends up as CO is dependent on the how well mixed the combustion is and is sensitive to the timing and fuel-air ratio. HC in the exhaust is thought to be due largely to unburnt fuel, which had dissolved in the cylinder oil film or been preserved in crevices (Flagan and Seinfeld, 1988).  $\text{NO}_x$  is an unavoidable product of high temperature combustion in air, increasing with combustion

temperature and favoured by fuel lean conditions. These considerations lead to the expectation that CO, HC and NO<sub>x</sub> emissions would be proportional in some way to fuel consumption with CO and HC showing more inter vehicle variation.

Similar considerations apply with respect to CO and NO<sub>x</sub> emissions from compression ignition (diesel) engines, except that combustion temperatures are not so high and the fuel is less well mixed with the air as burning fuel droplets are involved. With regard to HC emissions, any unburnt fuel is generally too involatile to be monitored, so that much less HC emission would be expected. Also, the diesel engine does not control air intake and hence, as there is excess air often present, this would favour NO<sub>x</sub> formation.

The following equations for SI exhaust emissions are from the work of Post et al., (1981) and Kent et al. (1982). The units for the following equations are g/min for the emissions and ml/min for fuel consumption, with the power in watts.

$$\text{CO} = 10.0 + 0.7 Z_t \quad (8)$$

$$\text{HC} = 0.70 + 0.07 Z_t \quad (9)$$

$$\text{NO}_x = 0.29 Z_t \quad (10)$$

In equations (6-10), if the acceleration term is such that  $Z_t$  is negative, then  $Z_t$  is set to zero.

We have developed similar formulations for SI and diesel vehicles, which have been matched to experimental data. They are:

$$\text{SI (no catalyst)} \quad \text{FC} = 9.9 \text{ EC} + 9 Z_t \quad (11)$$

$$\text{CO} = 1.65 \text{ EC} + 0.08 Z_t \quad (12)$$

$$\text{HC} = 0.165 \text{ EC} + 0.008 Z_t \quad (13)$$

$$\text{NO}_x = 0.004 \text{ EC} + 0.192 Z_t \quad (14)$$

## Light-duty diesel

$$FC = 9.9 EC + 6 Z_t \quad (15)$$

$$CO = 0.34 EC + 0.02 Z_t \quad (16)$$

$$HC = .136 EC + 0.008 Z_t \quad (17)$$

$$NO_x = 0.045 EC + 0.12 Z_t \quad (18)$$

## Heavy-duty diesel

$$FC = 9.9 EC + 6 Z_t \quad (19)$$

$$CO = 0.136 EC + 0.02 Z_t \quad (20)$$

$$HC = 0.136 EC + 0.008 Z_t \quad (21)$$

$$NO_x = 0.045 EC + 0.2 Z_t \quad (22)$$

In addition to the above equations, we have modelled cold start operation for SI vehicles. This is necessary when comparing model performance with test cycle emission data. Engine warm-up has been simulated by multiplying equations (12/12a) and (13/13a) by a factor,  $f_{cold}$ , given by

$$f_{cold} = 7 - 6 (1 - e^{-SF_n/t}) \quad (23)$$

where  $SF_n$  is the fuel consumed since engine start (ml) normalised to 2.5 l engine capacity and  $t$  is a characteristic warm-up time constant, chosen here to be 120 (s).

For catalyst-equipped vehicles a further factor,  $f_{cat}$ , which combines catalyst performance,  $E_{cat}$ , and warm up from cold start: This is applied to equations 11 -14.

$$SI \text{ (catalyst)} \quad FC = 9.7 EC + 8.8 Z_t \quad (11a)$$

$$CO = f_{cat} (1.65 EC + 0.08 Z_t) \quad (12a)$$

$$HC = f_{cat} (0.165 EC + 0.008 Z_t) \quad (13a)$$

$$NO_x = f_{cat} (0.004 EC + 0.192 Z_t) \quad (14a)$$

For CO and HC emissions, the catalyst efficiency,  $E_{cat}$  is given by:

$$E_{cat} = 0.5 - 0.4 \exp(-FC/120) \quad (24)$$

so that when combined with warm-up time we get:

$$f_{cat} = 1/(1+E_{cat}) e^{-SF_n/t} + E_{cat} \quad (25)$$

where the characteristic time is 1 min, as the catalyst warms up more rapidly than the engine and coolant systems.

For  $NO_x$  emissions:

$$E_{cat} = 0.5 \text{ for 3-way catalyst}$$

$$\text{or} \quad E_{cat} = 1 \text{ for oxidation catalyst} \quad (26)$$

The form of  $E_{cat}$  for CO and HC emissions in equation (25) is designed to reduce the catalyst efficiency as the exhaust flow rate increases and hence the residence time decreases. This appears necessary, based on the data of Carnovale et al., (1992), and which is discussed below. One of the limitations of FTP and related test cycles is that the absence of any high acceleration. This is particularly important in respect of catalyst equipped cars as, under these conditions, the engine management system goes into 'open loop' operation during which fuel rich conditions are allowed to prevail to prevent over heating of the catalyst. This can be simulated in the model by putting  $E_{cat} = 1$  when  $Z_t$  exceeds a certain value. In the work discussed here, this condition is not reached.

A feature of the current research is that we have measured excess atmospheric  $CO_2$  generated by the traffic, which can be directly related to fuel consumption. As nearly all the carbon in transport fuel is oxidised to  $CO_2$ , these emissions can be estimated directly from the fuel consumption:

$$CO_2 = M \rho F_c \quad (27)$$

where  $M$  is the ratio of the molecular weight of  $CO_2$  relative to molecular weight of the hydrocarbon fuel expressed per atom of C and  $\rho$  is the specific gravity of the fuel.



Allowance has been made for the carbon that ends up as CO or HC.

### 3.2.2 Validation Of Power - Based Emissions Model

The nature of the model is such that fuel consumption is the primary parameter evaluated and emphasis, therefore, must be placed on how well the model performs in this respect, although the main thrust of the model is to predict CO, HC and other pollutant emissions.

#### 3.2.2.1 Spark Ignition Vehicles

We have integrated equations (11) and (11a) over the ADR37A drive cycle to estimate fuel consumption rates for a number of in-use pre-1986 vehicles that were the subject of particle emission testing (Williams et al., 1987) and also a number of new post-1986 vehicles (SPCC, 1989). The results are compared to actual measurements in Figure 2. It can be seen that the model provides a reasonable estimate of fuel consumption for both the pre-1986 in-use vehicles and the post-1985 new vehicles. For post-1985 cars, used a value for  $C_d$  of 0.35 was chosen as opposed to 0.4 for the older vehicles.

The predicted CO, HC and NO<sub>x</sub> emissions from the pre-1986 SI vehicles are compared with the test data in Figures 3, 4 and 5 respectively, and those for the catalyst-equipped vehicles in Figures 6, 7 and 8. It can be seen that there is a large scatter in predicted v experimental emissions of CO and HC in the data leading to the above equations. This is common to all such databases as the minor exhaust components depend to a much greater extent on the condition and tune of the vehicle than does fuel consumption. However, overall, the predicted values were in the "ballpark". For the vehicles in the study of Williams et al., (1987), the predicted specific CO emissions (ie for unit (kg) fuel consumption) were in the range 100 - 250 g whilst the

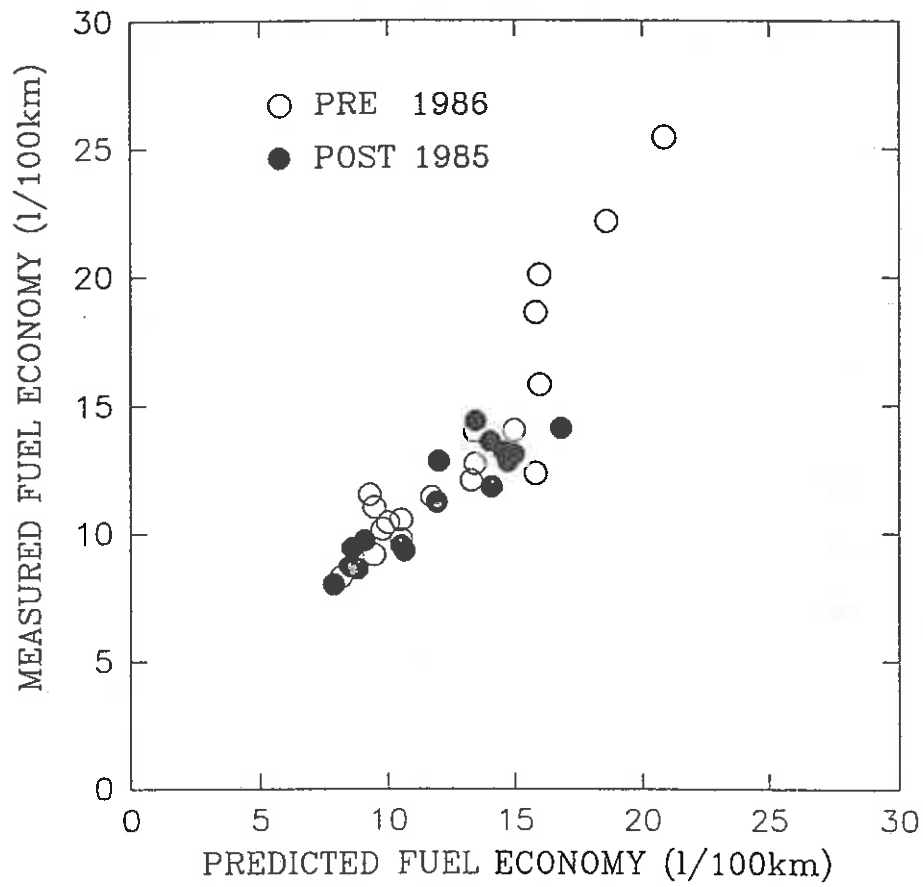


Figure 2. Comparison of predicted and measured ADR37 fuel economy for pre-1986 and post-1985 SI vehicles.

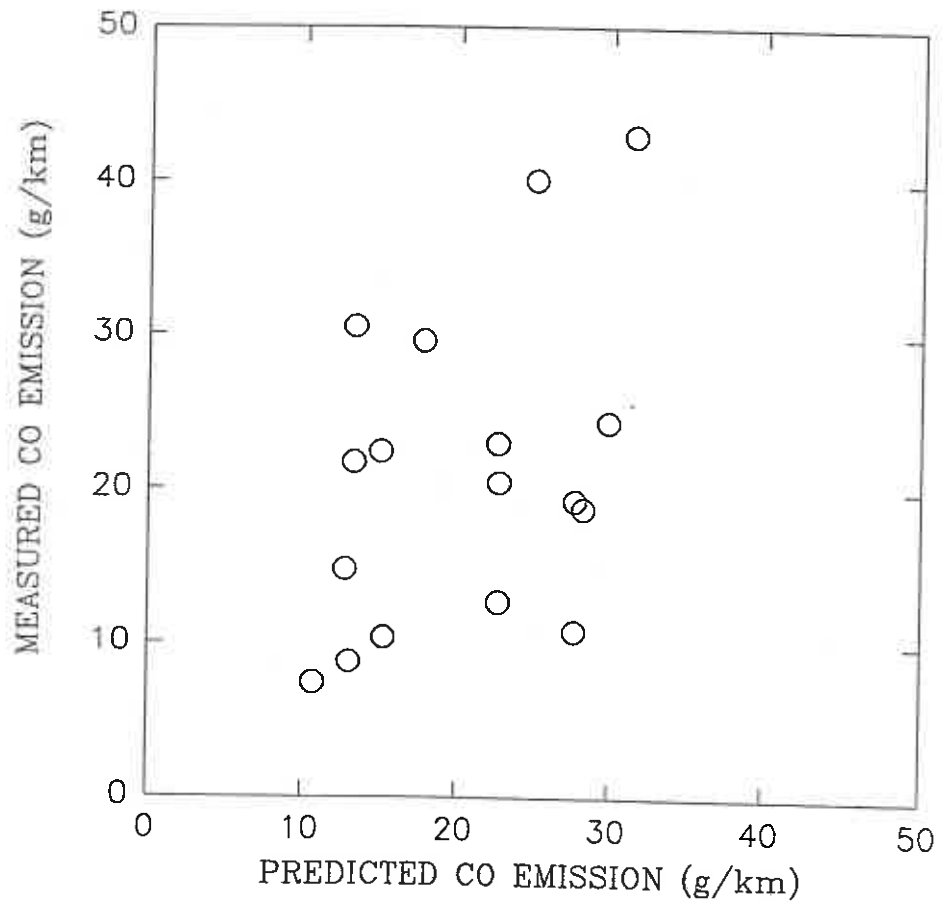


Figure 3. Comparison of predicted and measured ADR37 CO emissions for pre-1986 SI vehicles.

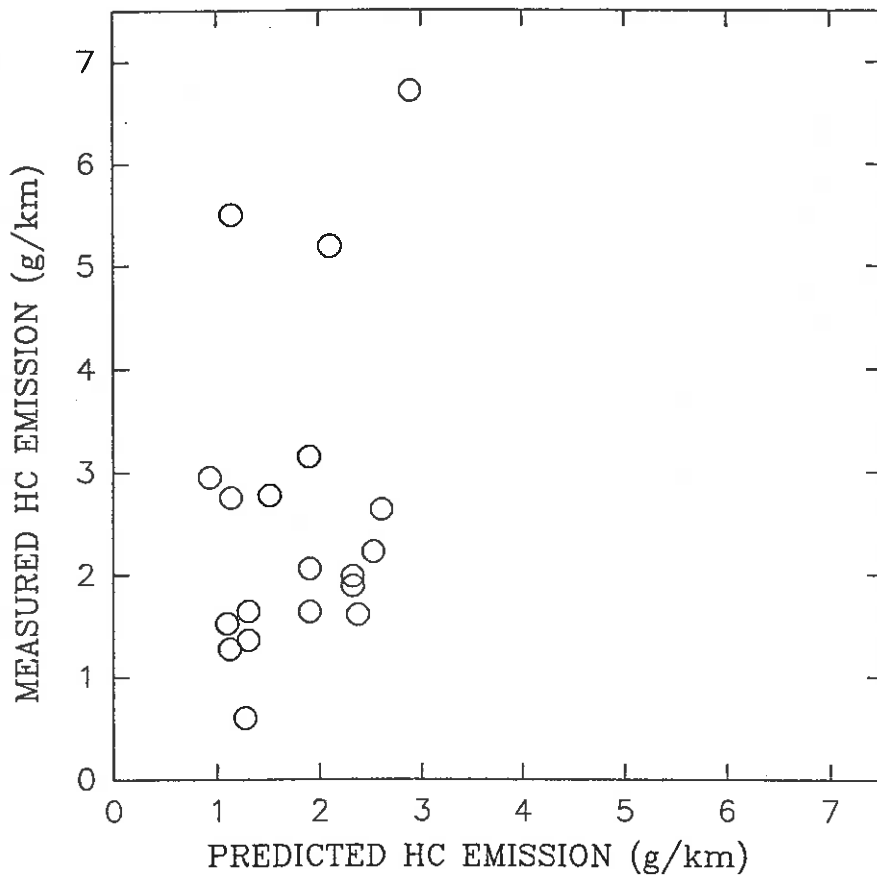


Figure 4. Comparison of predicted and measured ADR37 HC emissions for pre-1986 SI vehicles.

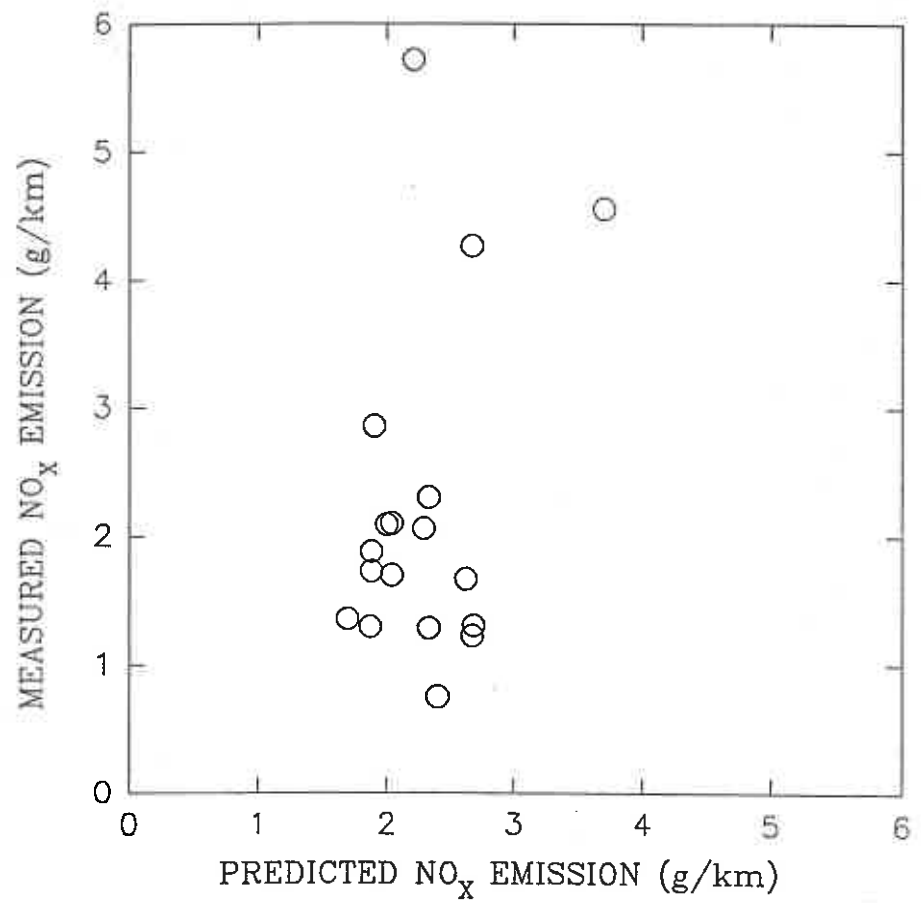


Figure 5. Comparison of predicted and measured ADR37 NO<sub>x</sub> emissions for pre-1986 SI vehicles..

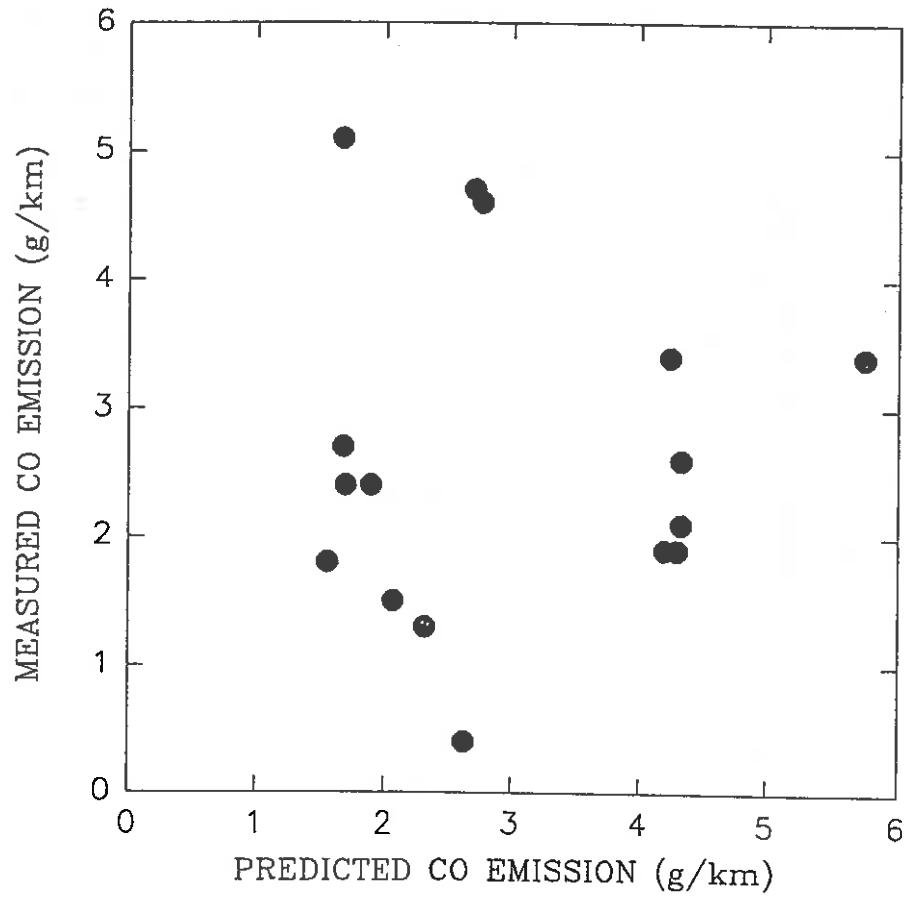


Figure 6. Comparison of predicted and measured ADR37 CO emissions for post-1985 SI vehicles.

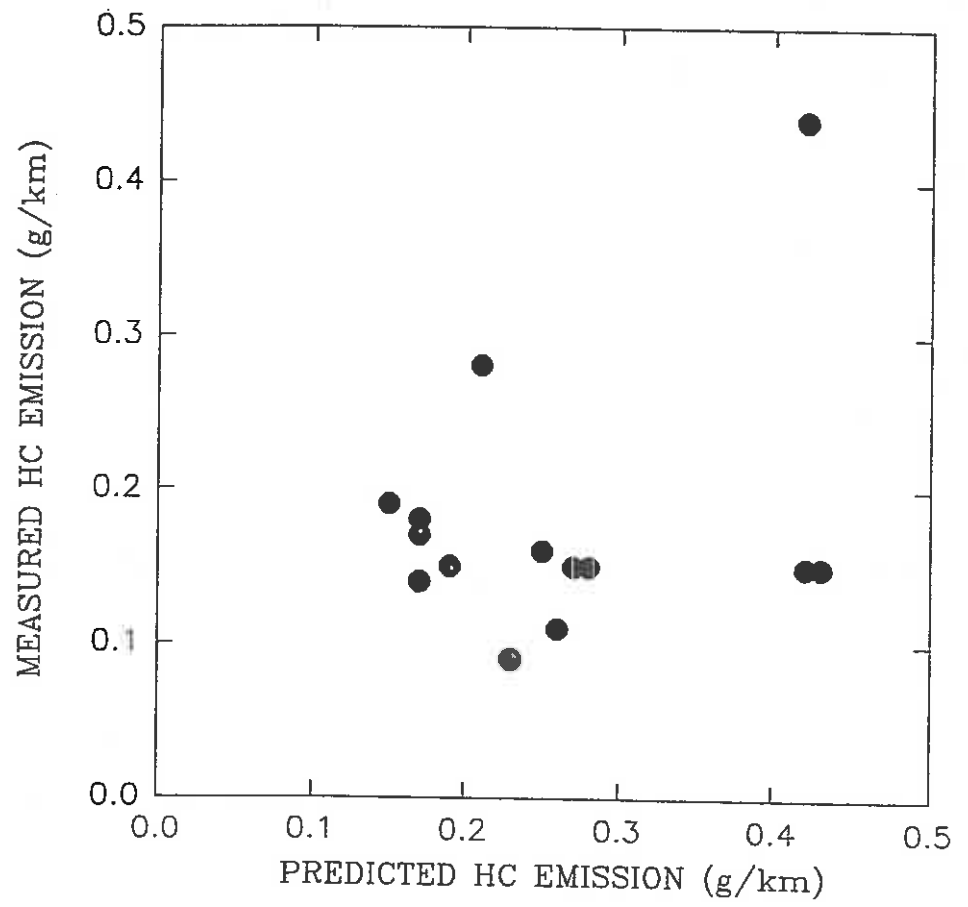


Figure 7. Comparison of predicted and measured ADR37 HC emissions for post-1985 SI vehicles.

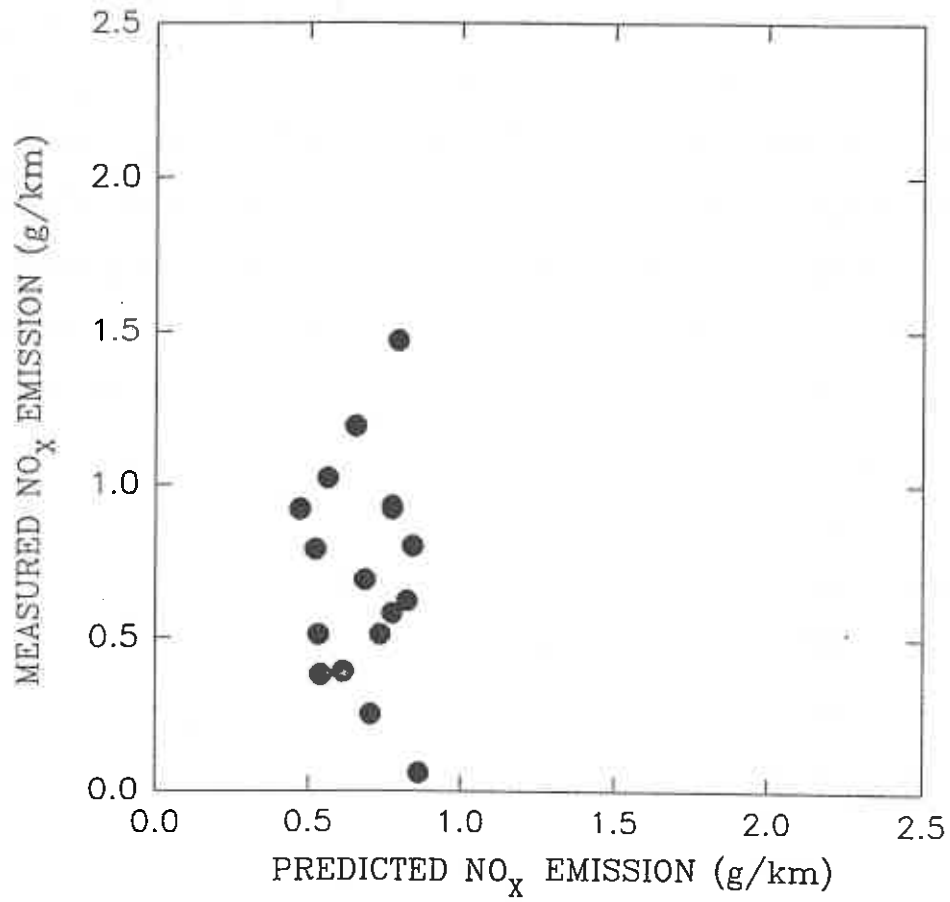


Figure 8. Comparison of predicted and measured ADR37 NO<sub>x</sub> emissions for post-1985 SI vehicles.



measured values were 100 - 400 g, the corresponding ranges for HC were 12 - 30 g versus 5 - 70 and for  $\text{NO}_x$ , 15 - 30 g versus 5 - 70 g.

Turning now to the work of Carnovale et al., (1992), who have measured emissions from over 1500 vehicles on a second by second basis over the ADR27 test cycle. These workers split up the test cycle into 3 modes consisting of freeway, arterial and congested segments, denoted by F, A and C in Figure 9 and binned the exhaust emissions accordingly. We have integrated the power model over these segments as well as the complete ADR27A test for a range of vehicles, and derived a fleet average emission rate comparable in vehicle make up to theirs. The results are compared with their test data in Table 1. Note the different trend in emission rates for CO and HC between the different technology groups as we move through the different road categories. For pre-1986 vehicles CO and HC emissions increase from freeway to congested conditions reflecting the increasing proportions of idle time, whereas this is not the case for catalyst equipped cars. It is this aspect that suggests that catalyst efficiency increases as vehicle speed decreases, (ie lower exhaust flow rate) that has led to equation (25).

### 3.2.2.2 Compression ignition (diesel) vehicles

Diesel vehicles are a significant traffic component but for which there is much less information on which to base an emission model. However, the general approach of estimating engine power demand should be equally applicable. The diesel engine is substantially more efficient than a petrol engine, so that the value for  $\beta$  is likely to be around 5 - 6 when estimating fuel consumption. The predicted fuel consumption (eqn 15) from some 18 in-use light duty diesel vehicles are compared with the data of Williams et al., (1987) in Figure 10. There is more scatter than for the SI vehicles, but agreement is still reasonable. Comparison of the predicted levels of CO, HC and  $\text{NO}_x$  emissions with measurements are shown in Figures 11, 12 and 13 respectively.

ADR27 TEST CYCLE

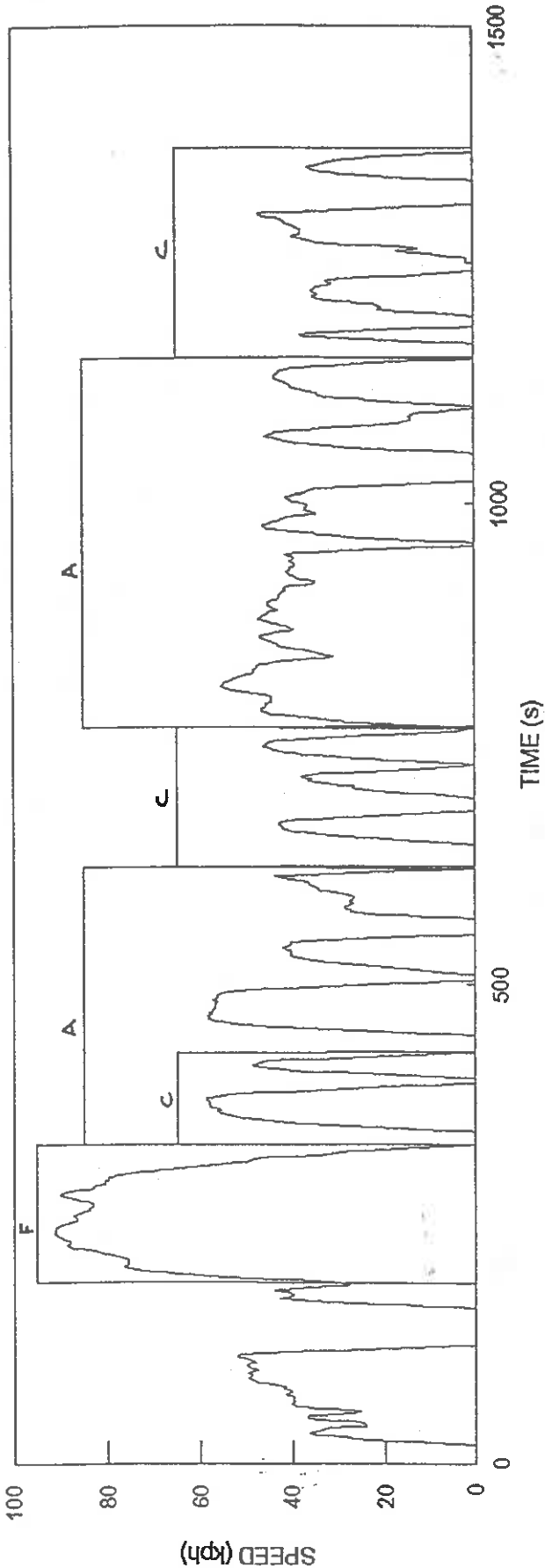


Figure 9. ADR27 drive cycle and it's division into freeway (F), arterial (A) and congested (C) segments.

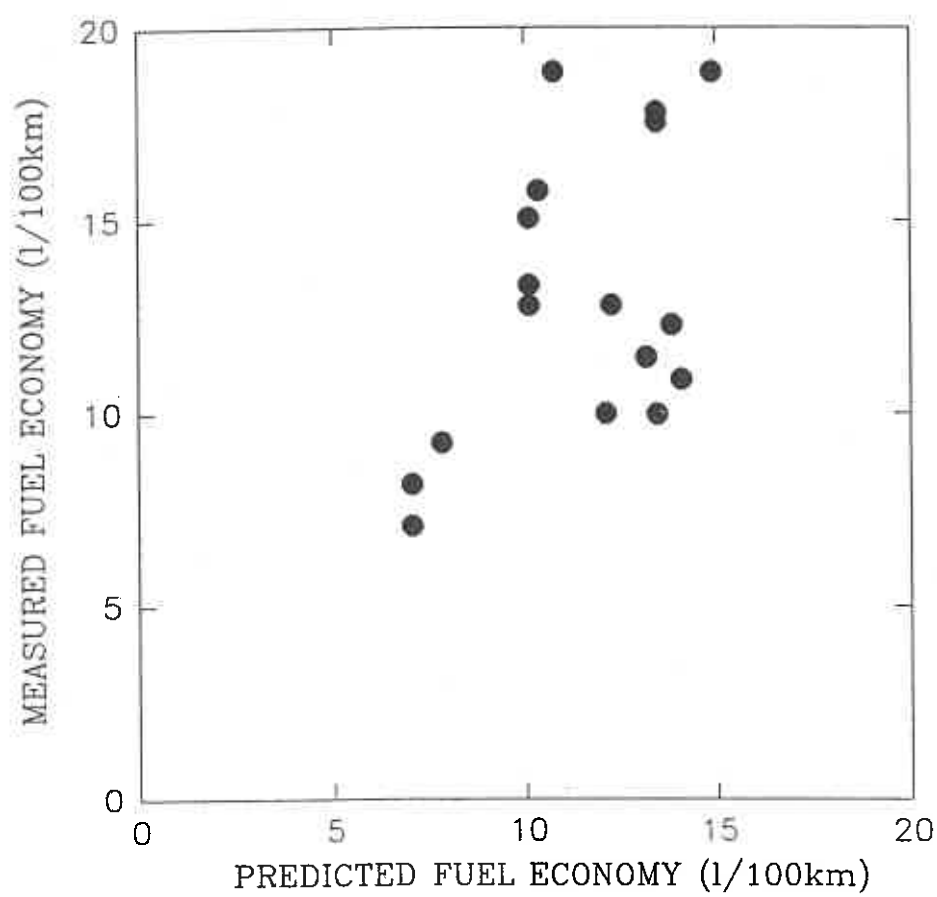


Figure 10. Comparison of predicted and measured ADR37 fuel economy for light-duty diesels.

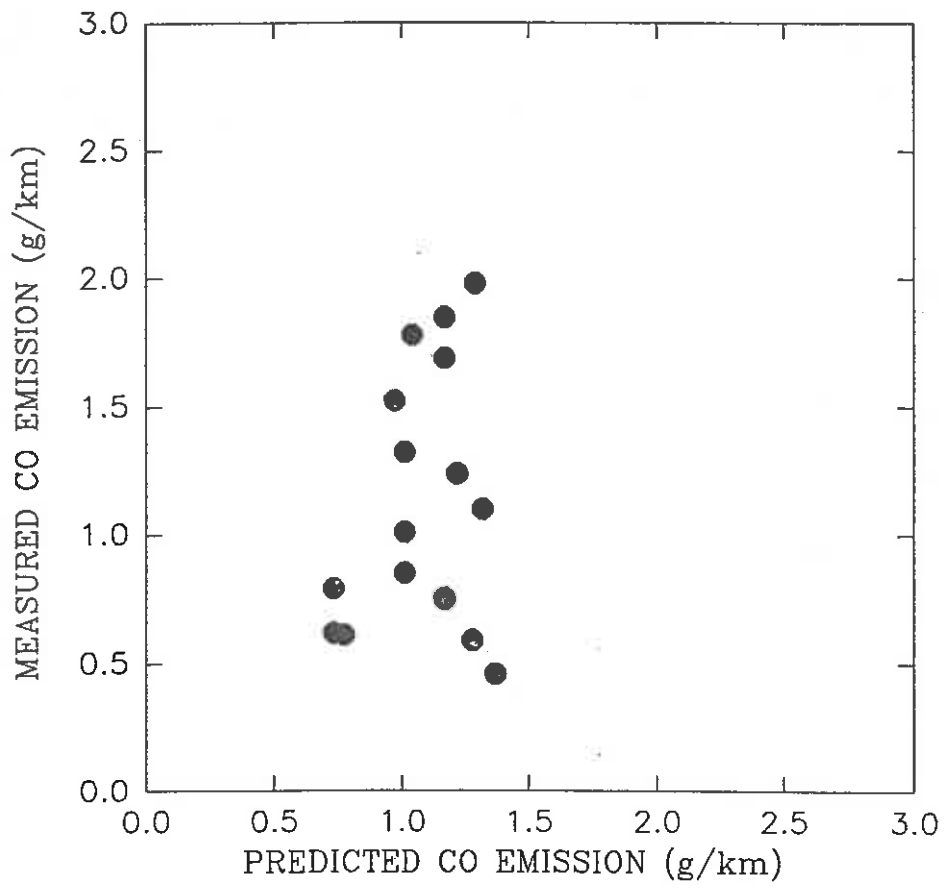


Figure 11. Comparison of predicted and measured ADR37 CO emissions for light-duty diesels.

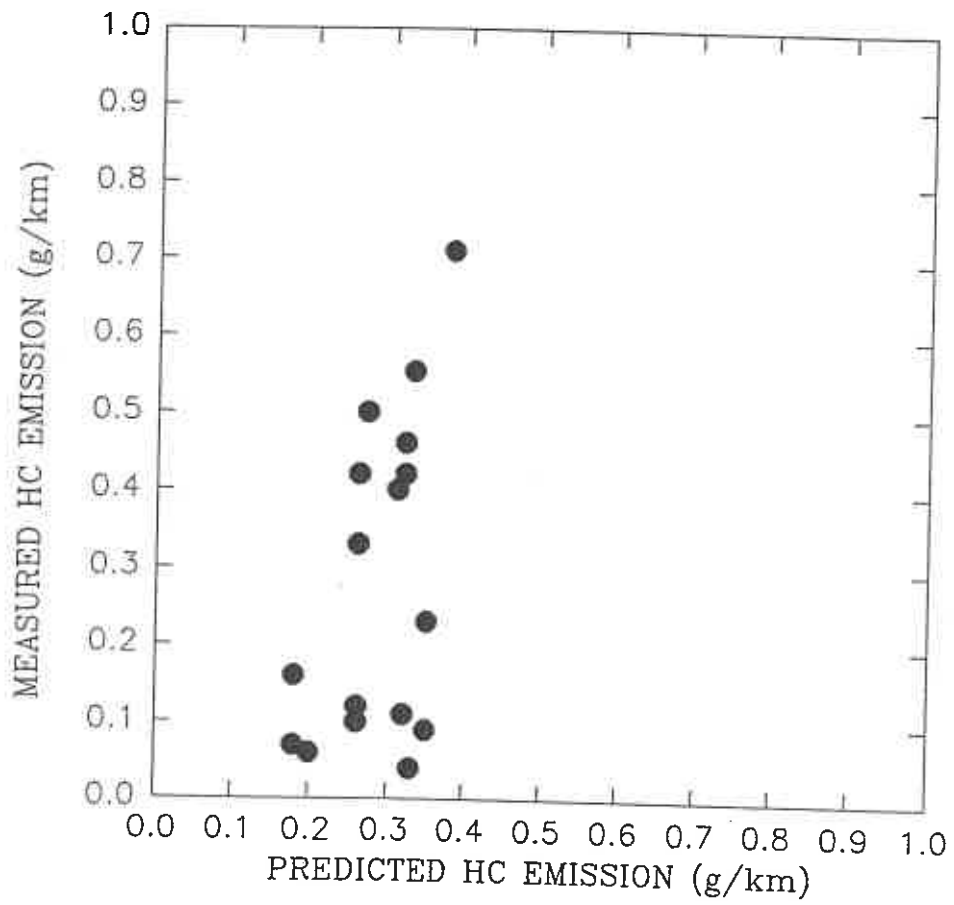


Figure 12. Comparison of predicted and measured ADR37 HC emissions for light-duty diesels.

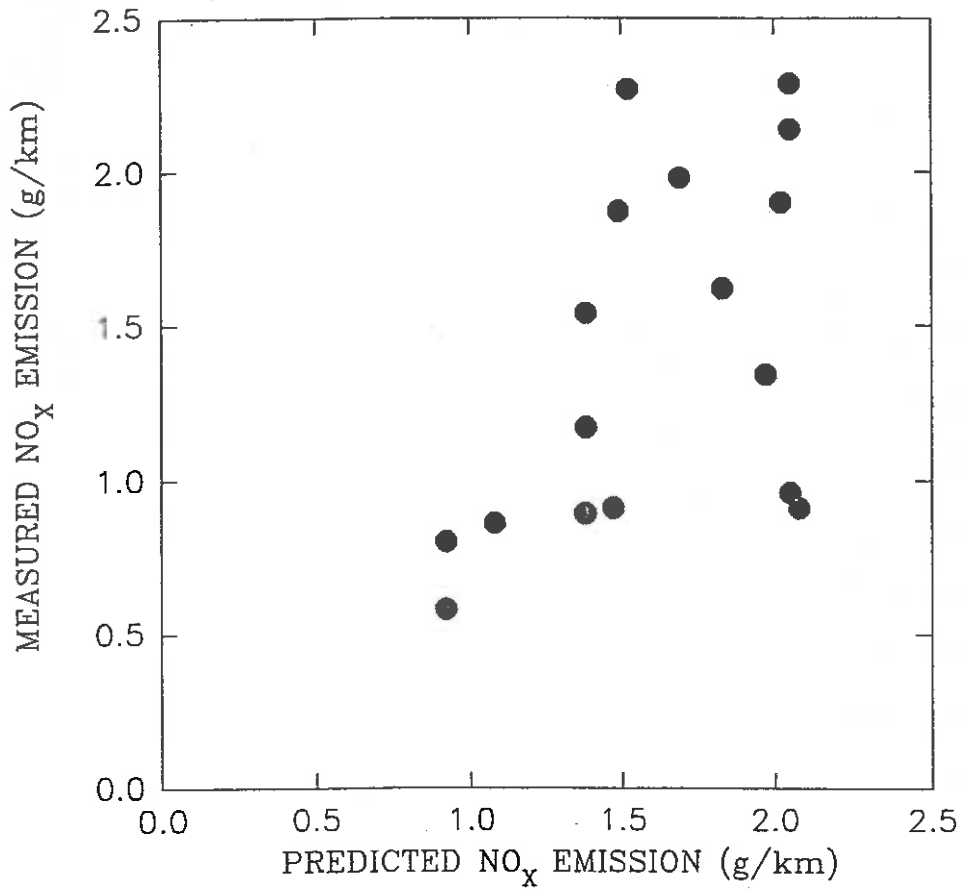


Figure 13. Comparison of predicted and measured ADR37 NO<sub>x</sub> emissions for light-duty diesels.

**TABLE 1. COMPARISON OF PREDICTED AND MEASURED EXHAUST EMISSIONS FOR PRE-1986 AND POST 1985 CARS**

	EMISSION RATES (g/km)			
	Pre - 1986		Post - 1985	
	Model	Measured	Model	Measured
<b>CO</b>				
Freeway	9.76	8.73	2.29	2.87
Arterial	12.89	13.04	2.16	2.35
Congested	18.78	19.58	3.00	3.38
ADR27A	20.30	19.30	5.36	6.56
<b>HC</b>				
Freeway	0.98	1.08	0.23	0.25
Arterial	1.29	1.37	0.21	0.20
Congested	1.88	2.09	0.30	0.32
ADR27A	2.03	1.76	0.53	0.31
<b>NO<sub>x</sub></b>				
Freeway	1.95	2.16	1.08	1.60
Arterial	1.77	1.20	1.05	0.87
Congested	2.17	1.64	1.31	1.10
ADR27A	2.04	1.54	1.20	1.17

A further evaluation of the model concerns how the emissions vary as a function of speed. This shown for catalyst-equipped vehicles for CO, in Figure 14 along with the US estimates for the 1990 SI vehicle fleet based on FTP data with SCF using the EMFAC-7F methodology of the California Air Resources Board. As the EMFAC-7F data are for a fleet average, we have added extra CO due to vehicle deterioration, as outlined in Table 9 (see Section 4), and assuming 60,000 km as the average odometer

## CO

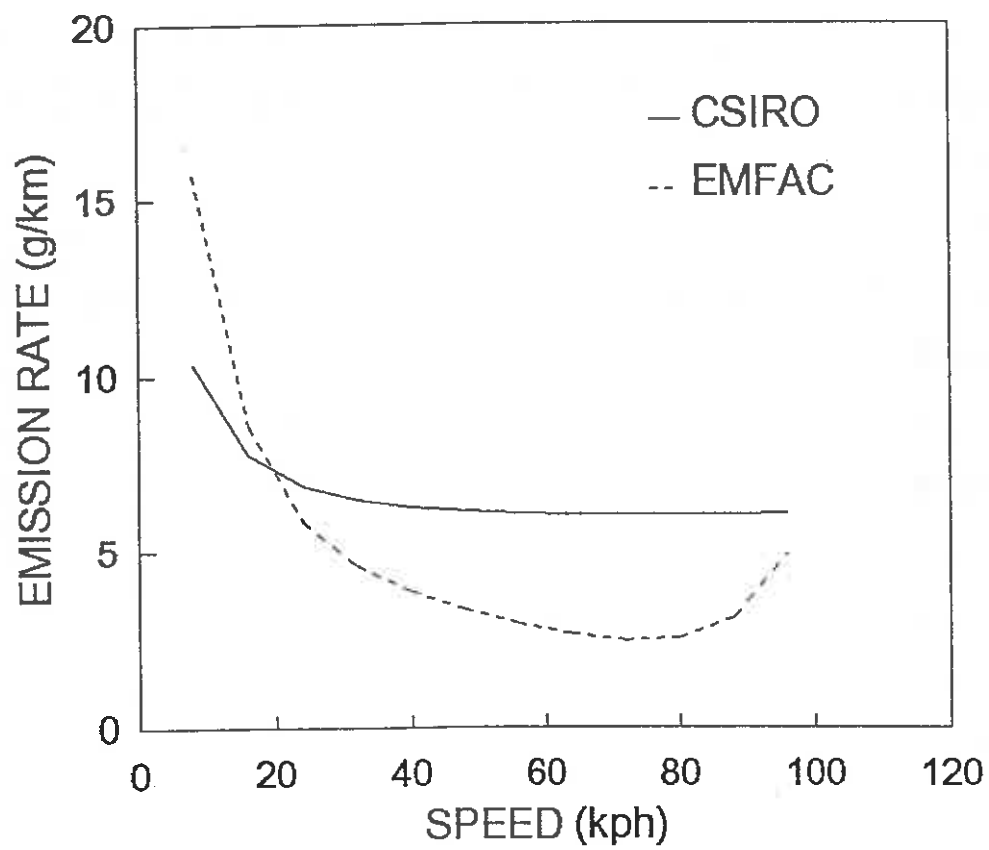


Figure 14. Comparison of predicted CO emission rate for 2.5 L unleaded SI vehicle with US EMFAC predictions as a function of speed.



reading. The results for HC and NO<sub>x</sub> are shown in Figures 15 and 16 respectively. It can be seen that the model produces curves which are similar in shape to the EMFAC produced curves but for CO is higher in value above 20 kph and higher throughout for NO<sub>x</sub>. This is due to a combination of different base emission rates and different deterioration factors/

One of the difficulties in trying to estimate fuel flow and emission rates for vehicles stems not only from the variability between vehicles, but also from the non-linear way these parameters are affected by vehicle speed and the dramatic influence of road slope. This is illustrated in Figure 17, which shows how the power demand and fuel consumption varies with vehicle speed and road slope for a car of all-up mass of 1430 kg. It can be seen that the extra power required to overcome a slope (or to carry out an acceleration manoeuvre) can easily double the fuel consumption rate. This is a major source of uncertainty in estimating traffic emissions.

### 3.3 DISPERSION MODELLING

We will now use the emissions model developed above in conjunction with models of atmospheric dispersion to assess the concentrations of traffic-generated pollution near major roadways.

In the current work four models of pollution from roadways have been examined. These models are ROADWAY, GM, HIWAY-2 and CALINE-4. One model, ROADWAY, which is a complex micro-meteorological model, requires some input data which are not routinely available and, as it did not perform well, has been dropped from further consideration. GM is the simplest of the three being just a line source in open terrain, whilst HIWAY will deal with a cut section of highway. CALINE, however, will model intersections, parking lots, multi-links etc and allow for NO<sub>2</sub> formation from reaction of NO with ambient O<sub>3</sub>. As CALINE is a more versatile

## HC

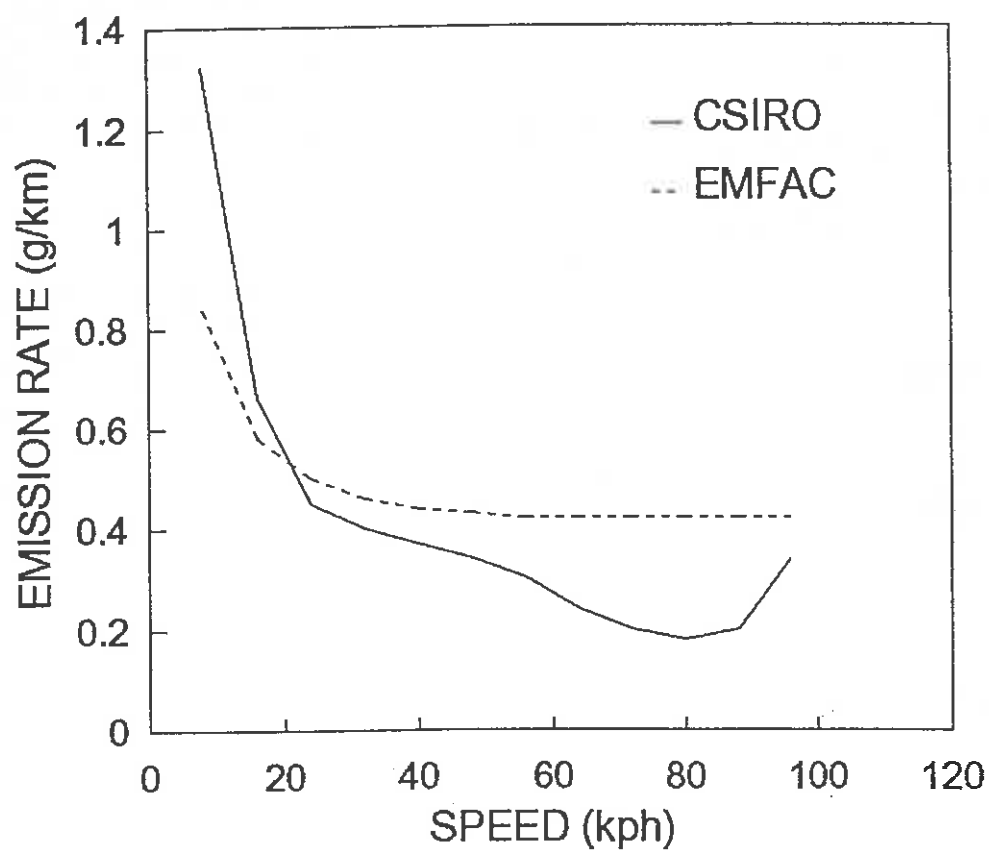


Figure 15. Comparison of predicted HC emission rate for 2.5 L unleaded SI vehicle with US EMFAC predictions as a function of speed.

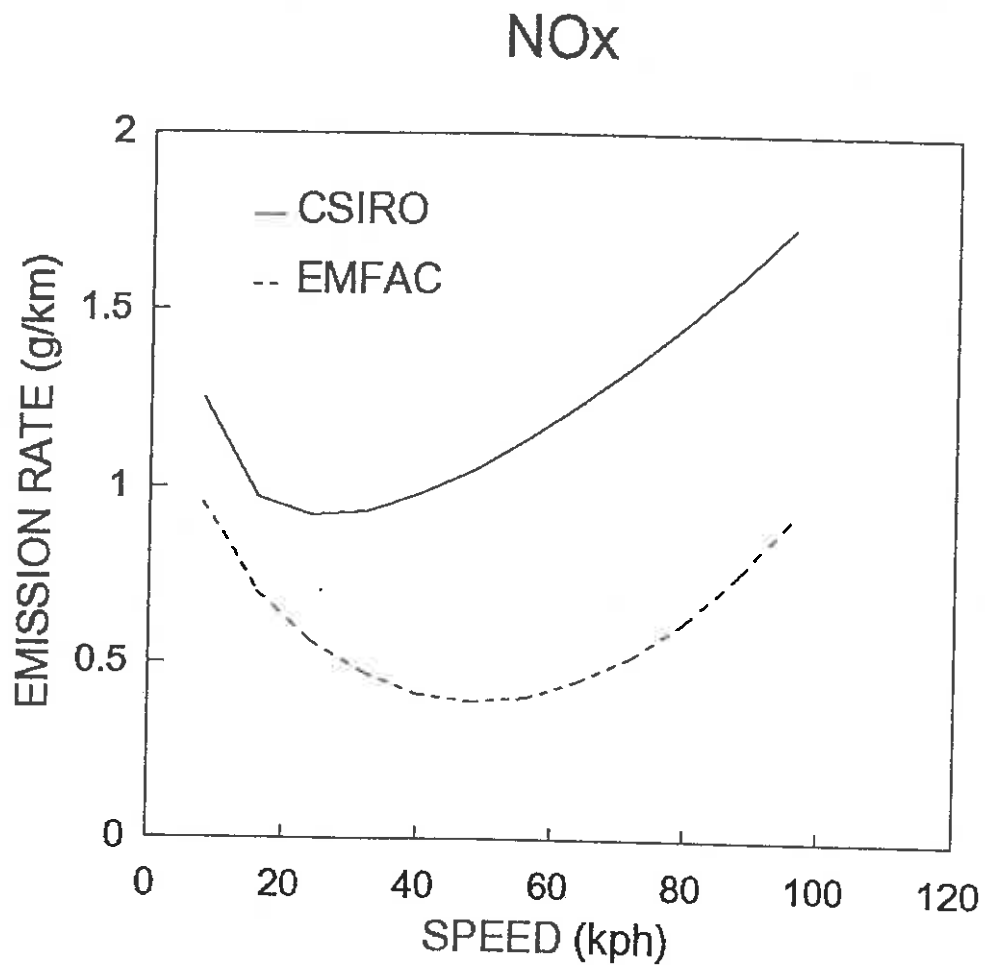


Figure 16. Comparison of predicted NO<sub>x</sub> emission rate for 2.5 L unleaded SI vehicle with US EMFAC predictions as a function of speed.

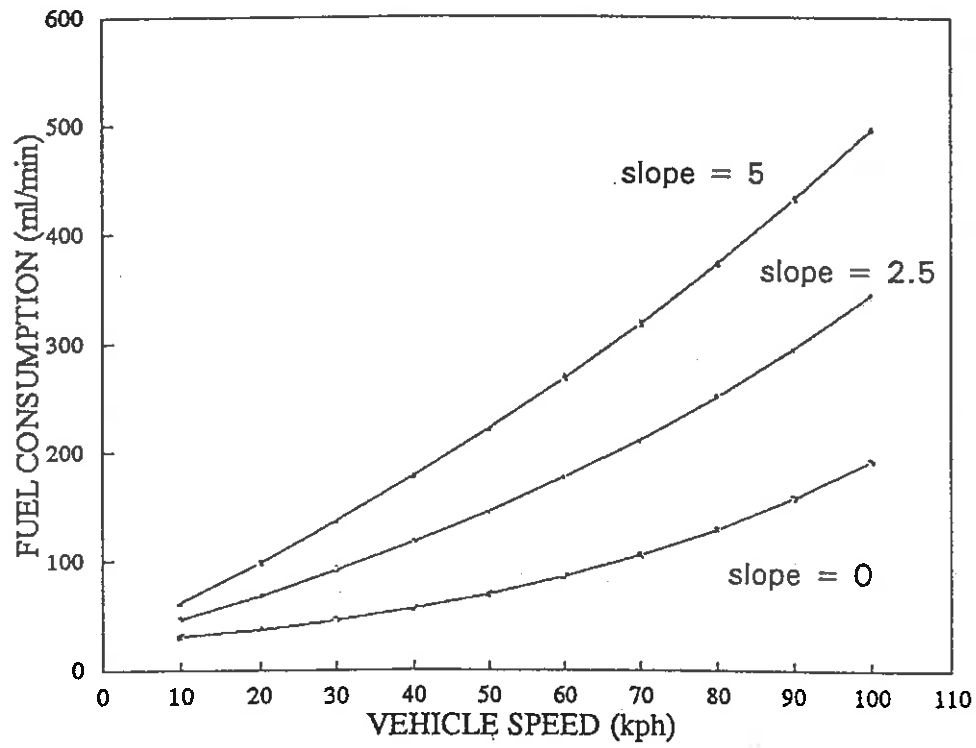
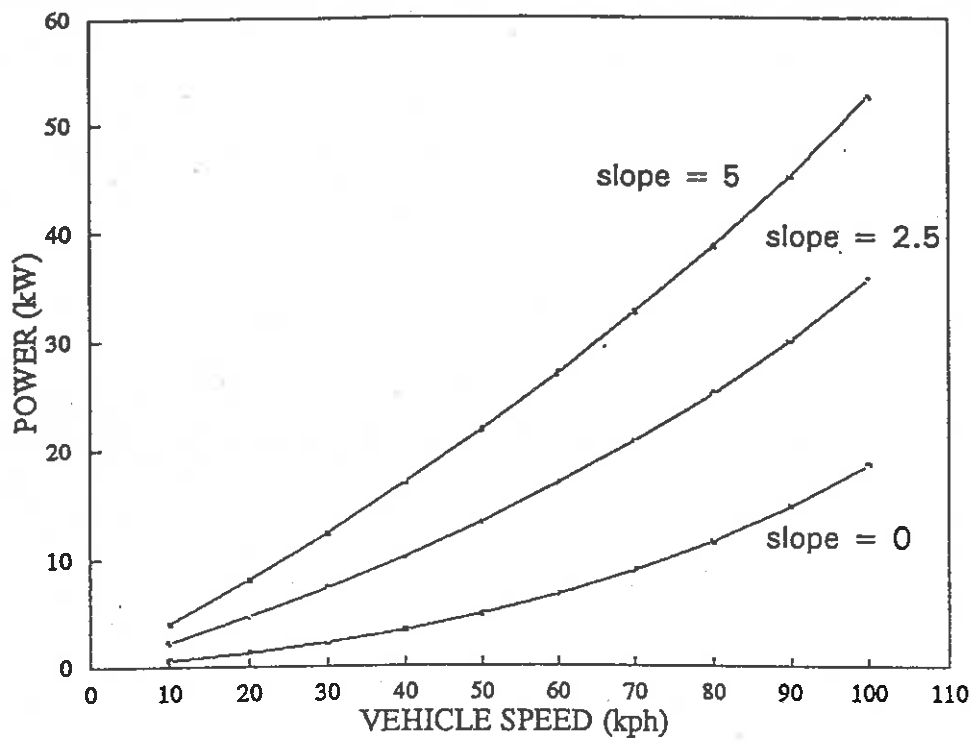


Figure 17. Effect of slope on power fuel consumption as a function of speed for 2.5L SI vehicle

program, and because there is often little to choose between properly formulated Gaussian dispersion models, much attention is given to CALINE.

Each of the models is available publicly and pre-existing computer code for ROADWAY, HIWAY-2 and CALINE-4 was used. The GM model code was written by CSIRO according to the prescription of Chock (1978), and is referred to, hereafter, as CHOCK. An outline of the model formulations follows.

### 3.3.1 CHOCK

The CHOCK model was developed by Chock (1978) and is a simple Gaussian line source model.

The concentration  $C(x,z)$  is given by

$$C(x,z) = \frac{Q}{\sqrt{2\pi} u \sigma_z} \left\{ \exp \left[ -\frac{1}{2} \left( \frac{z+h_e}{\sigma_z} \right)^2 \right] + \exp \left[ -\frac{1}{2} \left( \frac{z-h_e}{\sigma_z} \right)^2 \right] \right\}$$

where  $Q$  is the line source strength ie emission rate per unit length,  $u$  the effective crossroad wind component,  $\sigma_z$  the vertical dispersion parameter,  $x$  the distance from the receptor to the line source,  $z$  the height of the receptor relative to the ground,  $h_e$  the plume centre line height.

The CHOCK model develops parameters for input to equation above so that the model can be applied to oblique wind conditions without the explicit use of a  $\sigma_y$  term. The effect of lateral dispersion is taken into account by the  $\sigma_z$  term which is taken to be wind direction dependent. Also an empirical wind speed correction term is used to allow for the vehicle wake generated advection term. Details of the parameters as a function of stability conditions are to be found in Chock (1978).

Specifically the term for  $\sigma_z$  used in the GM model is

$$\sigma_z = (a+b f(\theta) x)^c$$

where  $a$ ,  $b$  and  $c$  are functions of atmospheric stability. The function  $f(\theta)$  is simply taken to be

$$f(\theta) = 1 + \beta \left| \frac{\theta - 90^\circ}{90^\circ} \right|^\gamma$$

where  $\beta$  and  $\gamma$  are given by Chock (1978) as a function of stability and  $\theta$  is the angle between the wind and the road.

Formulations are also included for the plume rise of the buoyant exhaust. Although, as pointed out by Chock, plume rise is not expected to be significant when the crossroad wind speed is  $>1\text{ms}^{-1}$ .

### 3.3.2 HIWAY-2

In HIWAY-2, a continuous line source is simulated by a series of point sources with the total contribution of sources integrated at the receptor. HIWAY-2 assumes that the vertical dispersion of the pollution from a roadway is given by a Gaussian distribution. As in all Gaussian modelling the effects of atmospheric turbulence are contained implicitly in the dispersion coefficients  $\sigma_y$  and  $\sigma_z$ , which are functions of atmospheric stability. The original formulation did not include the effects on the dispersion coefficients of vehicle generated turbulence. Rao and Keenan (1980) addressed this limitation by re-evaluating the vertical dispersion coefficient and substituting this for the Pasquill-Gifford curves which had been used previously. They included the effects of wake generated turbulence on the dispersion coefficient by simply adding it to the dispersion due to ambient turbulence,

i.e. 
$$\sigma_z^2 = \sigma_{zw}^2 + \sigma_{za}^2$$

where  $\sigma_{zw}^2$  is the variance due to wake effects and  $\sigma_{za}^2$  the variance due to atmospheric turbulence. Rao and Keenan (1980) derived an empirical relation for the wake generated dispersion and use this in HIWAY-2. These authors show that HIWAY-2

with the improved dispersion curves performed better than the earlier forms of dispersion coefficient used in the model.

### 3.3.3 CALINE-4

CALINE-4 is a line source model developed by the California Department of Transport. It divides the highway being considered into a series of elements each representing a section of the road. The concentration at the receptor from all relevant upwind elements are added and the total concentration calculated. Effectively the model replaces the highway by a series of equivalent finite line sources.

The region directly above the highway is treated as a zone of uniform emissions and turbulence. This is done in order to better approximate the nature of the emissions which are dispersed by wake turbulence as well as the buoyancy of the hot exhaust.

The initial vertical dispersion is modelled as a function of residence time within the initial turbulence region. ie

$$\sigma_z = 1.5 + 0.1t_r$$

where  $t_r$  is the residence time and is a simple function of the wind speed and highway width. The complete vertical dispersion parameter is computed in a manner to allow smooth transition between the initial value and the Pasquill- Gifford curve values at 10 km downwind.

The effects of roadway turbulence and heat flux on the spreading are assumed to operate for part of the distance downwind leading to enhanced dispersion. The horizontal dispersion coefficient is obtained directly from the formulation due to Draxler (1976) in which

$$\sigma_y = \sigma_\theta \times f(T/t_L)$$

where  $\sigma_\theta$  is the standard deviation of the horizontal wind angle,  $x$  is downwind distance,  $T$  is the travel time and  $t_L$  is the Lagrangian time scale. CALINE-4 uses Draxler's (1976) parameterization of  $t_L$  and his suggestion for the effect of wind shear on  $\sigma_z$  at greater distances.

### 3.4 MODEL PERFORMANCE

Each of the models has been evaluated using the experimental field data acquired as part of this project. The results from a set of seven experiments have been analysed in detail and utilised in this way, the set being chosen on a quality basis, when data recovery was highest. The emissions model is based on estimating fuel consumption, which exhibits much less inter-vehicle variability than CO, HC or NO<sub>x</sub> emission rates. Consequently, the dispersion models have been evaluated on the basis of CO<sub>2</sub> emissions.

The data used are for March 5, May 5, May 6, May 26, June 16 1992 and January 13 and April 6 1993. The data sets are listed in Tables 2 - 8 respectively. In estimating emission source strengths, it has been assumed that unleaded vehicles made up 55% of the passenger / light duty vehicle fleet, which in turn had an average engine capacity of 2.5L, an average mass of 1430 kg and an aerodynamic factor,  $C_dA$ , having a value of 0.73 m<sup>2</sup>. The corresponding values for heavy good vehicles (HGV) were 4L, 10,000 kg and 3.6 m<sup>2</sup>.

The emission strengths for the northbound and southbound directions were calculated for each period according to the measured traffic flow, vehicle mix and wind speed and direction. Deterioration factors for CO and HC were imposed on petrol-fuelled vehicles chosen from the data outlined in Carnovale et al., (1992), with the higher



**TABLE 2. DATA SUMMARY - 5 MARCH 1992 - EPPING HWY***Fixed sampling point*

START TIME	Concentrations (ppm)				WS	ANG	DIST	HT
	CO	CO <sub>2</sub>	NO <sub>x</sub>	HC				
16:00	1.8	12.0	0.140	0.234	2.0	79	2.0	2.5
16:30	0.7	10.1	0.126	0.156	2.5	84	2.0	2.5
17:00	1.4	10.3	0.134	0.131	2.5	79	2.0	2.5
17:30	1.2	10.0	0.130	0.140	2.0	77	2.0	2.5

*Mobile sampling point*

START TIME	Concentrations (ppm)				DIST	HT
	CO	CO <sub>2</sub>	NO <sub>x</sub>			
16:00	1.2	6.5	0.060		2.0	7.5
16:30	1.1	3.3	0.045		2.0	10.0
17:00	1.1	3.5	0.041		2.0	7.5
17:30	1.0	4.5	0.040		2.0	5.0

WS: wind speed (m/s), ANG : wind-road angle, DIST: distance from the road edge in metres, HT : height of the receptor in metres, all concentrations above background

**TRAFFIC STATISTICS**

START TIME	First Way (N)			Second Way (S)		
	NV	% HGV	V (kph)	NV	% HGV	V (kph)
16:00	1292	3.79	61.3	931	3.65	59.7
16:30	1460	2.67	61.3	970	3.29	59.7
17:00	1470	2.38	61.3	1063	2.53	59.5
17:30	1377	1.45	61.3	955	2.51	59.5

NV is the number of vehicles in the timeslot, V is the average velocity

**TABLE 3. DATA SUMMARY - 5 MAY 1992 - EPPING HWY***Fixed sampling point*

START TIME	Concentrations (ppm)				WS	ANG	DIST	HT
	CO	CO <sub>2</sub>	NO <sub>x</sub>	HC				
14:10	1.1	6.0	0.084	0.070	2.5	75.0	30.0	2.5
15:00	1.3	5.6	0.096	0.089	2.4	82.4	30.0	2.5
15:10	1.1	5.5	0.097	0.098	2.5	98.0	30.0	2.5
15:30	1.8	7.5	0.117	0.100	2.1	91.0	30.0	2.5
16:00	2.0	7.7	0.127	0.165	2.1	88.0	30.0	2.5
16:30	1.6	9.7	0.131	0.180	2.1	88.0	30.0	2.5
16:40	1.2	9.0	0.137	0.165	1.4	96.0	30.0	2.5

*Mobile sampling point*

START TIME	Concentrations (ppm)			DIST	HT
	CO	CO <sub>2</sub>	NO <sub>x</sub>		
14:10	1.9	10.0	0.194	2.0	2.5
15:00	1.5	7.1	0.158	15.0	2.5
15:10	1.0	5.5	0.104	30.0	2.5
15:30	0.8	5.0	0.111	45.0	2.5
16:00	0.7	4.0	0.103	60.0	2.5
16:30	2.0	13.3	0.185	2.0	2.5
16:40	1.6	10.0	0.164	15.0	2.5

WS: wind speed (m/s), ANG : wind-road angle, DIST: distance from the road edge in metres, HT : height of the receptor in metres, all concentrations above background

**TRAFFIC STATISTICS**

START TIME	First Way (N)			Second Way (S)		
	NV	% HGV	V (kph)	NV	% HGV	V (kph)
14:00	397	4.78	61.1	220	4.09	57.9
14:10	2116	3.78	61.1	1488	3.49	57.9
15:00	435	3.44	61.1	340	4.41	57.9
15:10	960	3.02	61.1	676	3.25	57.9
15:30	1452	2.41	61.1	998	3.71	57.9
16:00	1464	2.52	61.1	974	3.08	57.9
16:30	485	2.26	61.1	326	2.75	57.9

NV is the number of vehicles in the timeslot, V is the average velocity

**TABLE 4. DATA SUMMARY - 6 MAY 1992 - EPPING HWY***Fixed sampling point*

START TIME	Concentrations (ppm)				WS	ANG	DIST	HT
	CO	CO <sub>2</sub>	NO <sub>x</sub>	HC				
16:20	1.25	7.5	0.103	0.105	1.85	49	30.0	2.5
16:40	1.4	10.0	0.164	0.154	1.25	38	30.0	2.5
17:00	1.5	9.0	0.098	0.125	1.80	47	30.0	2.5
17:20	1.8	10.0	0.104	0.122	1.70	47	30.0	2.5

*Mobile sampling point*

START TIME	Concentrations (ppm)				DIST	HT
	CO	CO <sub>2</sub>	NO <sub>x</sub>			
16:20	1.15	8.5	0.115		30.0	2.5
16:40	1.60	12.0	0.255		15.0	2.5
17:00	1.90	14.5	0.204		2.0	2.5
17:20	1.00	8.0	0.085		60.0	2.5

WS: wind speed (m/s), ANG : wind-road angle, DIST: distance from the road edge in metres, HT : height of the receptor in metres, all concentrations above background

**TRAFFIC STATISTICS**

START TIME	First Way (N)			Second Way (S)		
	NV	% HGV	V (kph)	NV	% HGV	V (kph)
16:20	946	3.17	61.1	643	3.73	57.9
16:40	973	2.46	61.1	669	3.28	57.9
17:00	981	2.24	61.1	721	2.63	57.9
17:20	489	2.66	61.1	342	2.34	57.9

NV is the number of vehicles in the timeslot, V is the average velocity

**TABLE 5. DATA SUMMARY - 26 MAY 1992 - JAMES RUSE DRIVE***Fixed sampling point*

START TIME	Concentrations (ppm)				WS	ANG	DIST	HT
	CO	CO <sub>2</sub>	NO <sub>x</sub>	HC				
8:00	1.7	14.5	-----	-----	2.0	59	27.0	2.5
8:30	1.65	13.5	0.203	-----	1.9	57	27.0	2.5
9:20	1.2	10.0	0.205	-----	1.9	72	27.0	2.5
9:50	1.4	12.0	0.180	-----	1.8	28	27.0	2.5
10:10								

*Mobile sampling point*

START TIME	Concentrations (ppm)				DIST	HT
	CO	CO <sub>2</sub>	NO <sub>x</sub>			
8:00	2.4	23.3	0.348		4.0	2.5
8:30	1.3	10.0	0.174		57.0	2.5
9:10	2.3	18.8	0.279		4.0	2.5
9:20	1.6	10.0	0.195		27.0	2.5
9:50	1.3	7.4	0.164		57.0	2.5
10:10	2.1	15.5	0.183		4.0	2.5

WS: wind speed (m/s), ANG : wind-road angle, DIST: distance from the road edge in metres, HT : height of the receptor in metres, all concentrations above background

**TRAFFIC STATISTICS**

START TIME	First Way (S)			Second Way (N)		
	NV	% HGV	V (kph)	NV	% HGV	V (kph)
8:00	1391	5.82	39.7	822	12.04	50.7
8:30	1487	5.51	45.3	936	11.21	57.7
9:10	1514	7.86	50.0	1035	13.72	57.7
9:20	327	11.93	33.3	205	14.15	57.7
9:50	820	11.22	47.6	652	17.18	57.7
10:10	568	11.80	50.0	385	17.14	57.7

NV is the number of vehicles in the timeslot, V is the average velocity

**TABLE 6. DATA SUMMARY - 16 JUNE 1992 - JAMES RUSE DRIVE***Fixed sampling point*

START TIME	Concentrations (ppm)				WS	ANG	DIST	HT
	CO	CO <sub>2</sub>	NO <sub>x</sub>	HC				
8:00	2.2	21.0	0.282	.....	1.6	68	30.0	2.5
8:40	1.8	16.3	0.259	.....	1.7	63	30.0	2.5
9:10	1.6	16.0	0.243	.....	1.8	64	30.0	2.5
9:30	1.5	13.0	0.247	.....	1.6	60	30.0	2.5
10:00	1.7	11.3	0.177	.....	1.5	60	30.0	2.5
10:40	1.1	11.5	0.118	.....	1.5	63	30.0	2.5

*Mobile sampling point*

START TIME	Concentrations (ppm)				DIST	HT
	CO	CO <sub>2</sub>	NO <sub>x</sub>			
8:00	1.8	12.0	0.280		15.0	10.0
8:40	2.7	22.8	0.367		1.0	2.5
9:10	1.8	15.0	0.284		30.0	2.5
9:30	1.7	10.0	0.241		15.0	10.0
10:00	2.4	19.3	0.324		1.0	2.5
10:40	1.2	10.5	0.112		30.0	2.5

WS: wind speed (m/s), ANG : wind-road angle, DIST: distance from the road edge in metres, HT : height of the receptor in metres, all concentrations above background

**TRAFFIC STATISTICS**

START TIME	First Way (S)			Second Way (N)		
	NV	% HGV	V (kph)	NV	% HGV	V (kph)
8:00	536	4.10	47.5	279	11.82	50.1
8:40	2103	5.99	51.6	1259	10.17	57.2
9:10	1196	7.10	56.1	742	13.47	61.9
9:30	631	9.98	51.8	443	14.67	61.0
10:00	865	12.71	50.5	728	17.03	61.9
10:40	1199	11.92	52.8	1042	17.37	57.7

NV is the number of vehicles in the timeslot, V is the average velocity

**TABLE 7. DATA SUMMARY - 13 JAN 1993 - EPPING HWY***Fixed sampling point*

START TIME	Concentrations (ppm)				WS	ANG	DIST	HT
	CO	CO <sub>2</sub>	NO <sub>x</sub>	HC				
1:56	2.1	6.5	0.079	0.36	3.5	87.4	10.0	2.5
2:27	1.7	6.7	0.091	0.35	4.6	80.1	10.0	2.5
2:50	1.85	6.4	0.099	0.34	3.1	65.6	10.0	2.5
3:10	1.85	7.5	0.089	0.33	2.3	80.3	10.0	2.5
3:30	2.07	8.2	0.097	0.37	2.9	80.0	10.0	2.5
4:00	1.85	8.0	0.083	0.31	3.1	82.5	10.0	2.5
4:20	1.73	8.3	0.089	0.38	2.1	88.7	10.0	2.5
4:50	1.55	9.7	0.950	0.43	3.5	73.9	10.0	2.5

*Mobile sampling point*

START TIME	Concentrations (ppm)				DIST	HT
	CO	CO <sub>2</sub>	NO <sub>x</sub>			
1:56	1.4	4.7	0.036		10.0	10.0
2:27	1.6	5.1	0.051		10.0	7.0
2:50	1.7	5.7	0.091		10.0	4.0
3:10	1.5	6.4	0.069		10.0	7.0
3:30	1.0	5.4	0.068		10.0	10.0
4:00	1.4	6.4	0.052		10.0	7.0
4:20	1.6	6.7	0.066		10.0	4.0
4:50	1.0	5.3	0.052		10.0	10.0

WS: wind speed (m/s), ANG : wind-road angle, DIST: distance from the road edge in metres, HT : height of the receptor in metres, all concentrations above background

**TRAFFIC STATISTICS**

START TIME	First Way (N)			Second Way (S)		
	NV	% HGV	V (kph)	NV	% HGV	V (kph)
1:56	773	3.4	59.6	668	4.6	60.7
2:26	593	4.55	59.5	461	4.77	60.7
2:46	639	2.97	59.9	410	4.15	60.5
3:06	654	4.74	59.5	448	4.46	60.5
3:26	1170	4.10	59.5	674	3.41	60.5
3:56	900	2.22	59.5	414	2.65	60.5
4:16	1531	2.61	59.5	741	3.77	60.5
4:46	949	2.63	59.5	587	3.74	60.5

NV is the number of vehicles in the timeslot, V is the average velocity

**TABLE 8. DATA SUMMARY - 6 APRIL 1993 - HOMEBUSH***Fixed sampling point*

START TIME	Concentrations (ppm)				WS	ANG	DIST	HT
	CO	CO <sub>2</sub>	NO <sub>x</sub>	HC				
8:36	1.7	8.0	0.105	0.240	2.9	21	30.0	2.5
9:06	1.6	7.0	0.103	0.145	2.6	27	30.0	2.5
9:36	2.2	9.0	0.107	0.172	2.5	35	30.0	2.5
10:06	1.8	8.5	0.079	0.162	2.4	24	30.0	2.5
10:36	2.0	6.5	0.054	0.181	2.2	15	30.0	2.5
11:06	2.1	6.0	0.078	0.168	2.1	51	30.0	2.5

*Mobile sampling point*

START TIME	Concentrations (ppm)				DIST	HT
	CO	CO <sub>2</sub>	NO <sub>x</sub>			
8:36	2.05	13.0	0.124		1	2.5
9:06	1.20	6.0	0.073		55	2.5
9:36	2.40	15.0	0.125		1	2.5
10:06	1.70	7.0	0.071		30	5.0
10:36	1.10	4.0	0.054		4	6.0
11:06	2.20	12.5	0.076		1	2.5
11:36	1.50	4.5	0.064		55	2.5

WS: wind speed (m/s), ANG : wind-road angle, DIST: distance from the road edge in metres, HT : height of the receptor in metres, all concentrations above background

**TRAFFIC STATISTICS**

START TIME	First Way (N)			Second Way (S)		
	NV	% HGV	V (kph)	NV	% HGV	V (kph)
8:36	865	4.74	69.0	1022	7.04	68.5
9:06	777	6.17	69.0	762	10.49	68.5
9:39	612	7.35	69.0	674	12.61	68.5
10:10	576	10.94	69.0	518	10.62	68.5
10:41	491	8.55	69.0	577	9.01	68.5
11:12	550	8.54	69.5	547	8.95	68.5
11:42	485	4.21	69.5	462	8.44	68.5

NV is the number of vehicles in the timeslot, V is the average velocity

SPCC values used for pre-1986 and the USEPA values for later vehicles as summarised in Table 9. The deterioration factors used for  $\text{NO}_x$  emissions were lower than in Carnovale et al., (1992), as our base emission rate is higher. Running loss HC emissions were also added to the exhaust HC emissions according to USEPA recommendations. It was assumed that catalyst-equipped vehicles make up 55% of the SI fleet and that for 40% of such vehicles, the catalyst was of the three-way type.

Although each of the field locations was substantially flat, the effect of slopes of up to  $1.5^\circ$  imposed on each way was investigated, in order to account for a combination of non-zero slope and random vehicle acceleration manoeuvres. It should be noted that the effect of slope is to increase the vehicles' requirement for power, resulting in

**TABLE 9. DETERIORATION FACTORS FOR SI VEHICLES**

Deterioration factors (g/10,000 km)		
	Leaded	Unleaded
CO	1.60	0.78
HC	0.10	0.05
$\text{NO}_x$	0.015	0.005

increased  $\text{CO}_2$  and  $\text{NO}_x$  emission rates but has a much smaller influence on CO and HC emission rates as these pollutants are less power- sensitive. Typical emission quantities, predicted for each of the pollutants, are listed in Table 10 for two roads with different amounts of heavy (diesel) traffic, viz: Epping Highway and James Ruse Drive. It can be seen that the heavy traffic effects mostly the amounts of  $\text{CO}_2$  and  $\text{NO}_x$ .

The stability classes chosen to best represent the meteorology at any instance varied from Pasquill-Gifford category B (slightly unstable) to D (slightly stable). We consider



that these three classes cover most daytime periods in Sydney. Class D was used for early morning in the winter months, with C or B stability chosen for afternoon periods.

**TABLE 10. EXAMPLES OF VEHICLE AVERAGE EMISSION RATES**

	% HGV	Emission Rates (g/vehicle/km)			
		CO <sub>2</sub>	CO	HC	NO <sub>x</sub>
Epping Hwy	3.7	275	20	2.0	2.9
J. Ruse. Drive	17.0	405	19	1.9	4.4

Figures 18, 19, 20 and 21 present the comparison between measured and predicted CO<sub>2</sub> concentrations for all the data points for HIWAY and CALINE for slopes of 0°, 0.5°, 1.0° and 1.5° respectively. The results from HIWAY are plotted in each of these diagrams for comparison.

It is evident that, at zero slope, HIWAY performs fairly well but CALINE under-predicts, but CALINE is brought into line better by a slope of 0.5° or 1.0°. As has been pointed out there are reasons why some slope is to be expected. A plot of the predictions of CHOCK against the experimental data is given in Figure 22 for a slope of 1°. It is noteworthy there is more scatter from this model, believed to be due to poor treatment of the vertical dispersion. Although this problem can be easily overcome, through modification of the dispersion parameters used, we have not considered CHOCK further as it only has the capability to deal with simple links.

The data in Figures 18 - 21 have been obtained at different heights and distances from the roadside and over a range of wind-speeds, road-wind angles and atmospheric stability. The agreement between measured and predicted concentrations is remarkably good for atmospheric pollution studies. If we now look at a more restricted data set obtained at one height (2.5m) and at one distance (30m) and shown in Figures 23 for a slope of 0.5°, then the scatter is reduced.

# CO<sub>2</sub>

SLOPE = 0

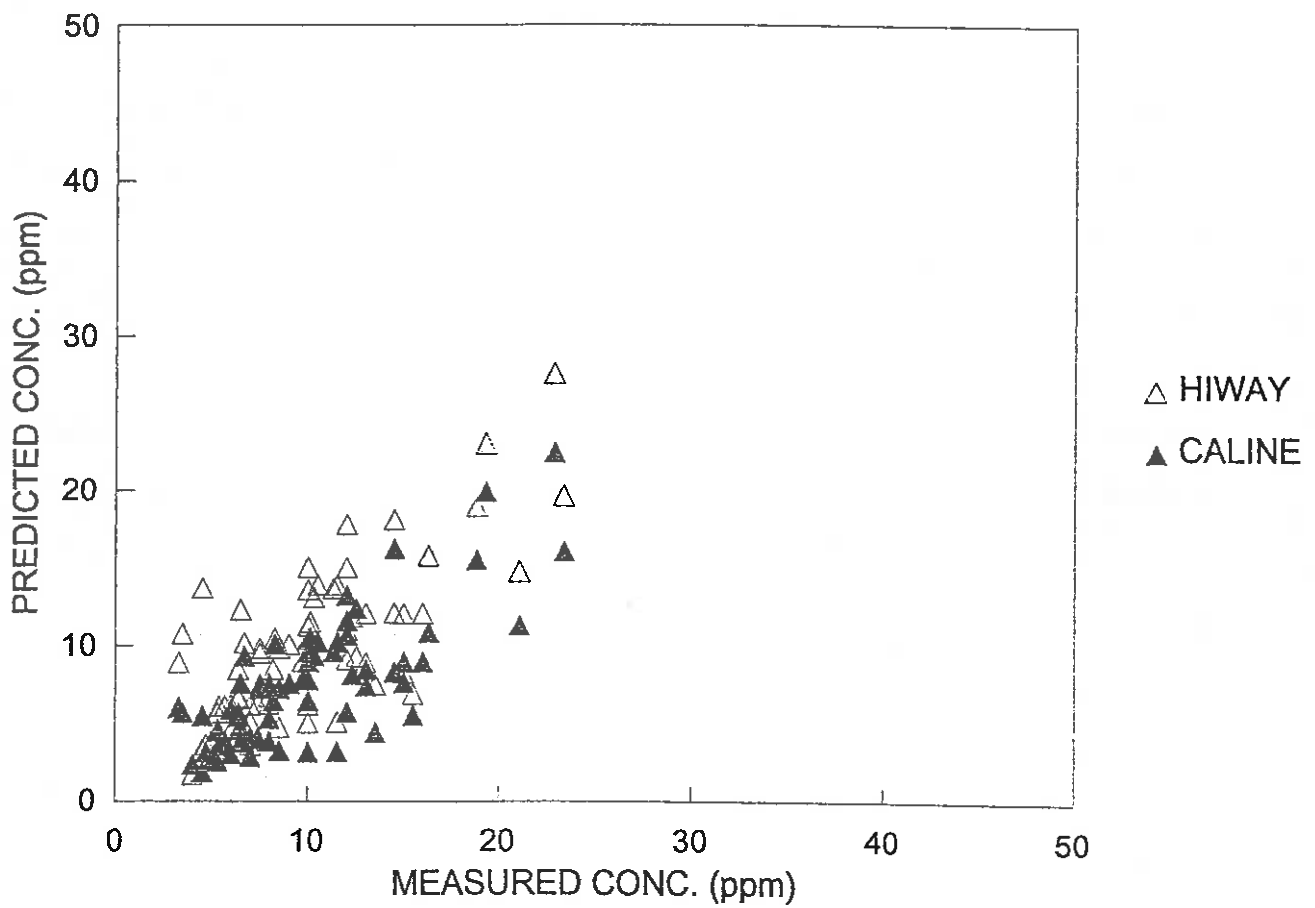


Figure 18. Predicted v measured CO<sub>2</sub> concentration for HIWAY and CALINE : slope = 0°.

CO<sub>2</sub>

SLOPE = 0.5

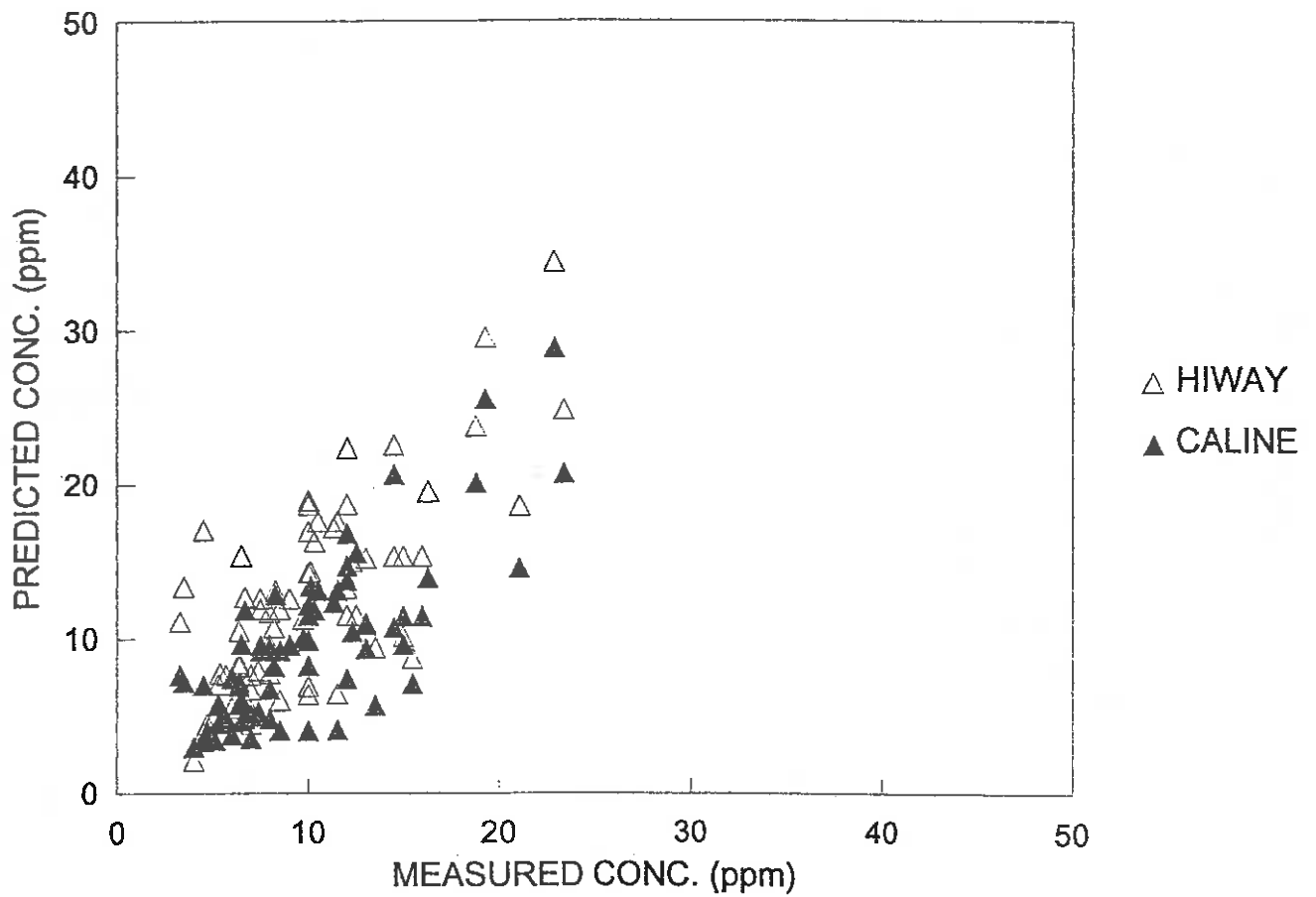


Figure 19. Predicted v measured CO<sub>2</sub> concentration for HIWAY and CALINE : slope = 0.5<sup>0</sup>.

# CO<sub>2</sub>

SLOPE = 1.0

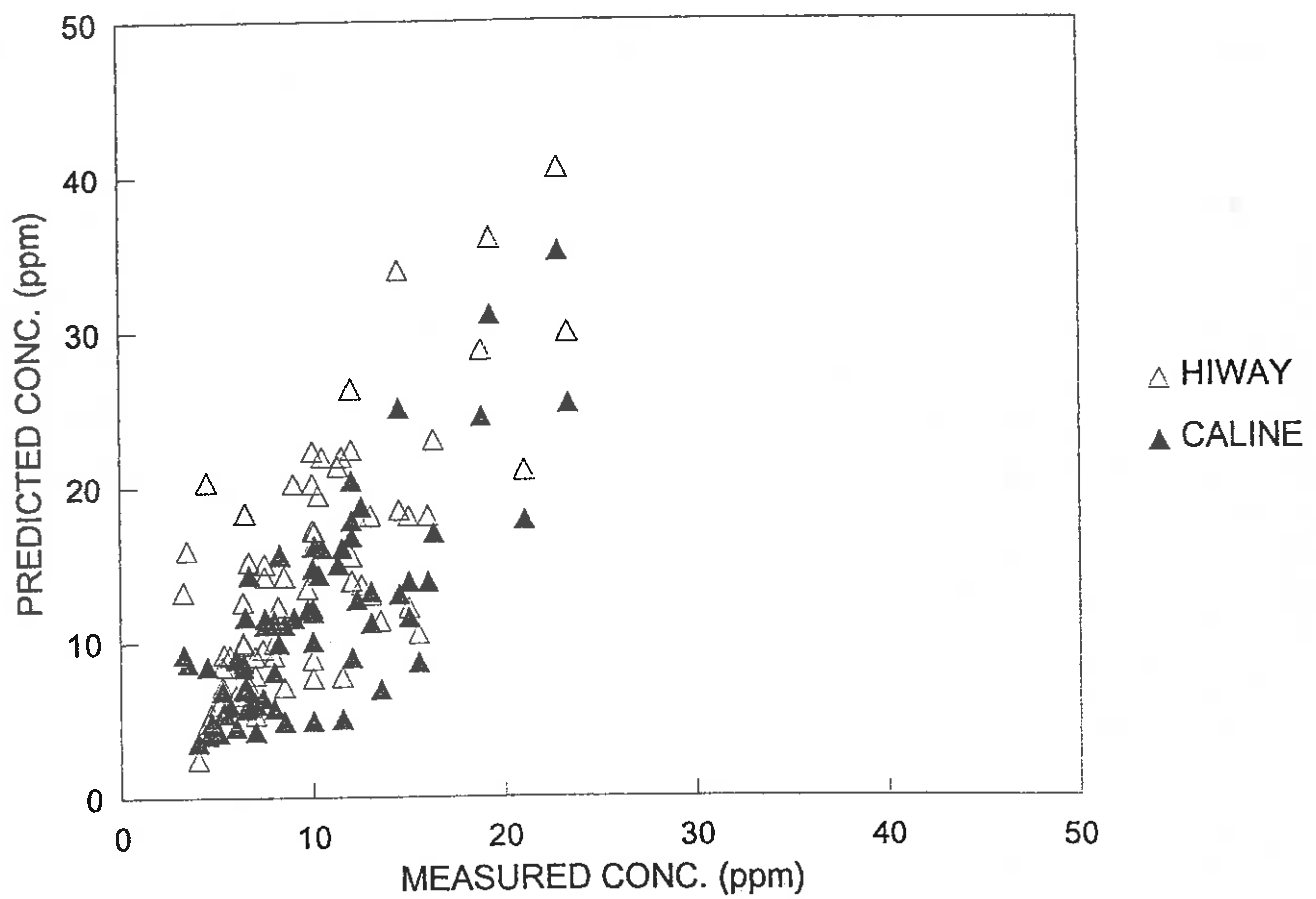


Figure 20. Predicted v measured CO<sub>2</sub> concentration for HIWAY and CALINE : slope = 1.0<sup>0</sup>.

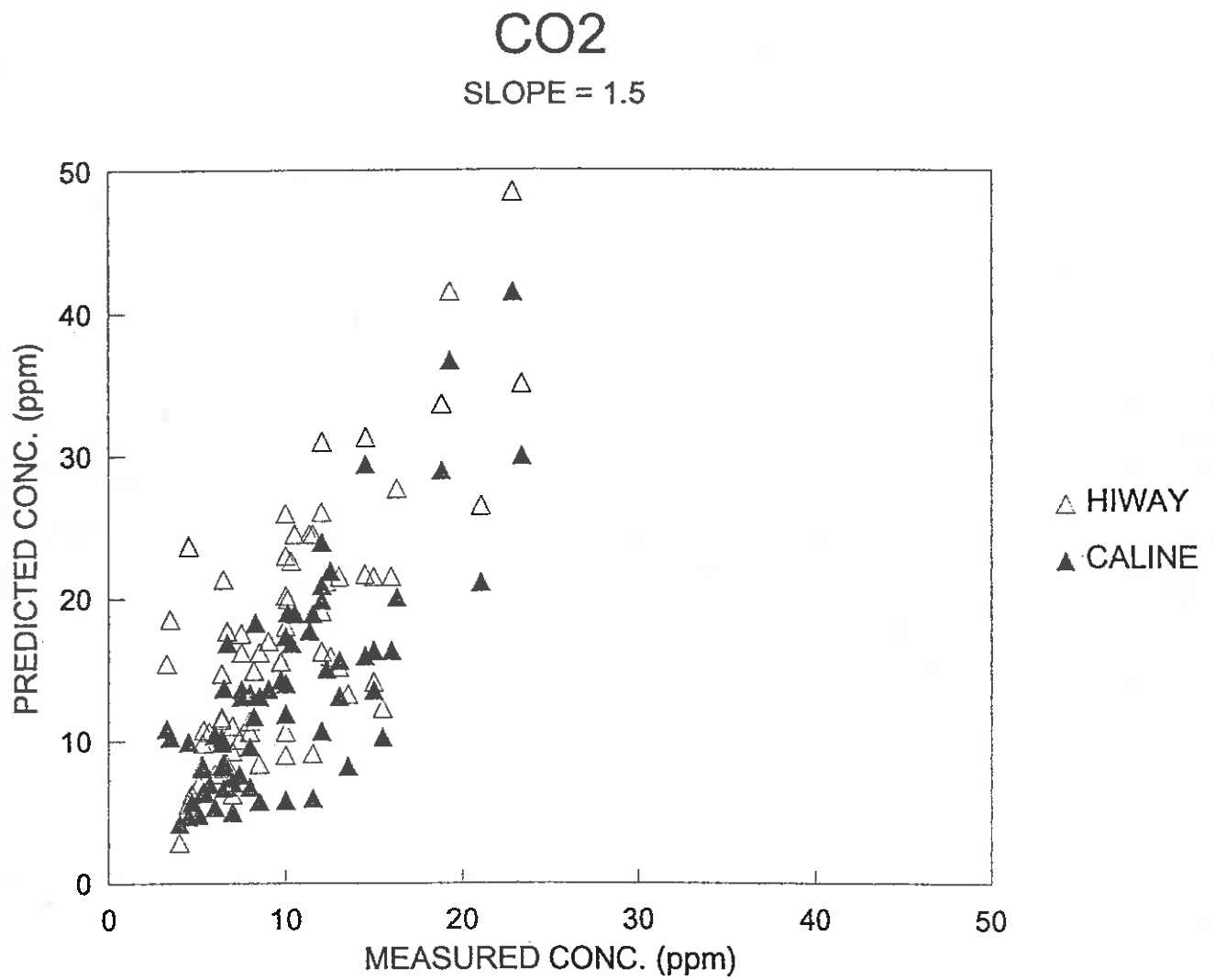


Figure 21. Predicted v measured CO<sub>2</sub> concentration for HIWAY and CALINE : slope = 1.5<sup>o</sup>.

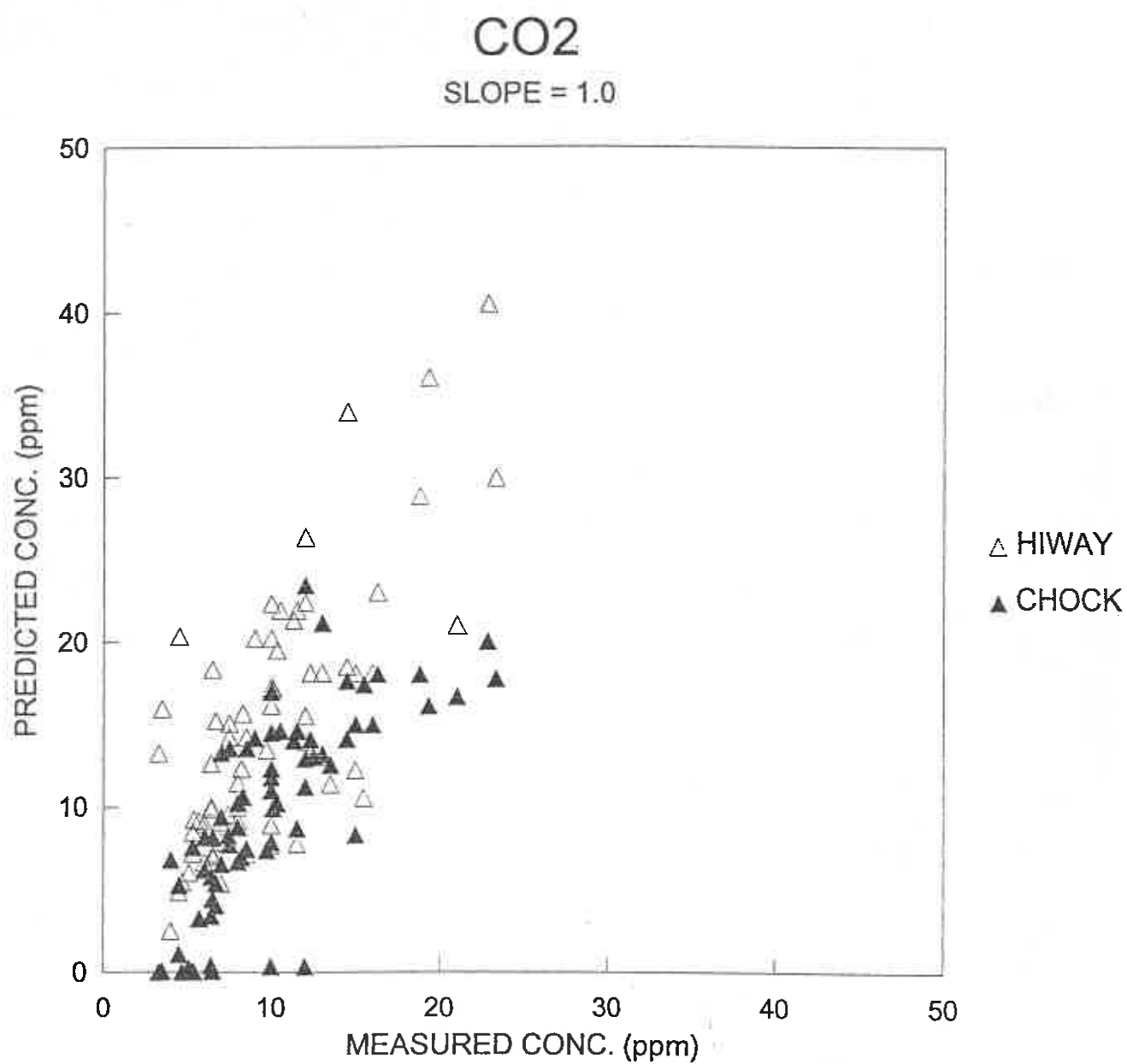


Figure 22. Predicted v measured CO<sub>2</sub> concentration for HIWAY and CHOCK: slope = 1.0<sup>0</sup>.

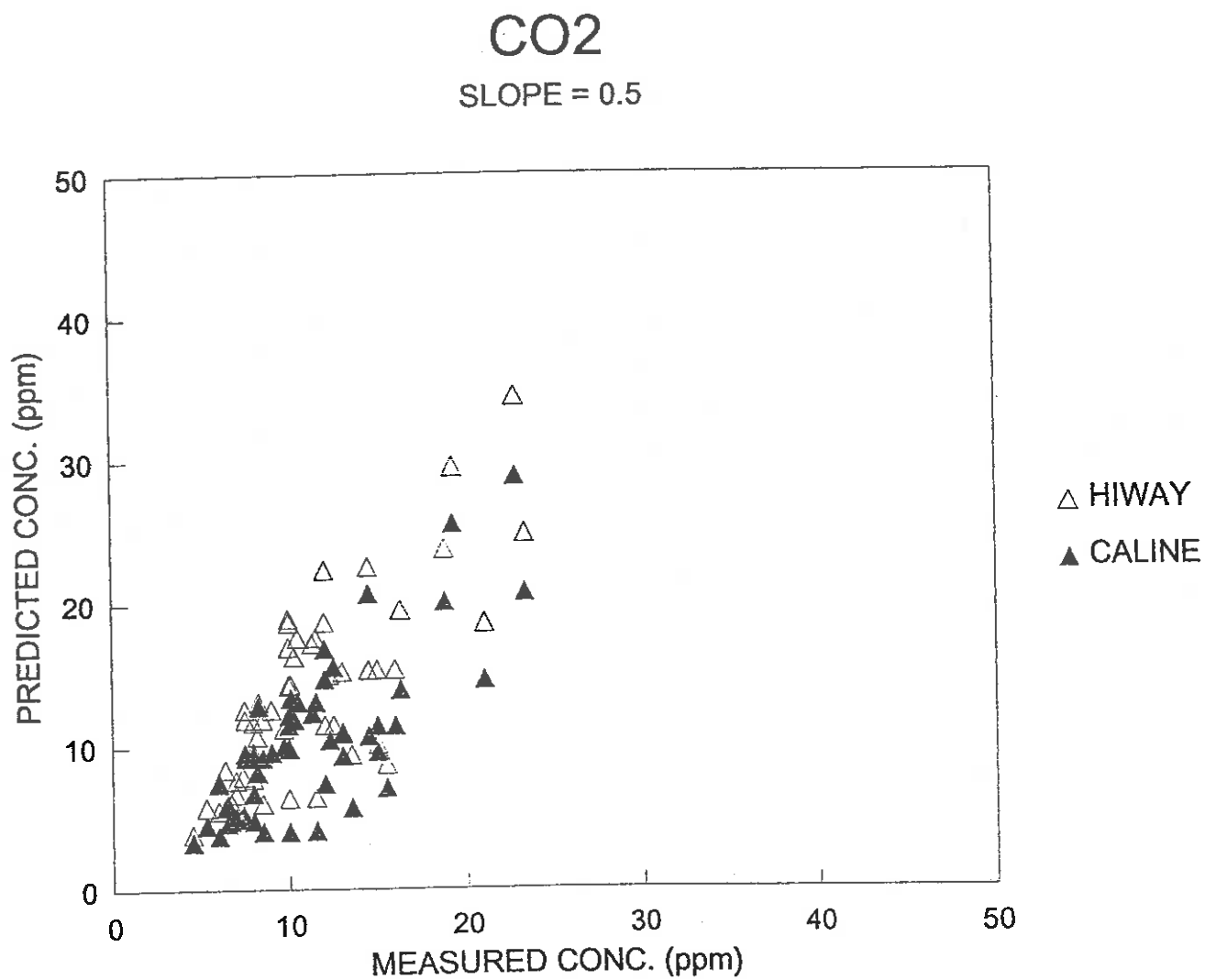


Figure 23. Predicted v measured CO<sub>2</sub> concentration for HIWAY and CALINE : slope = 0.5°. sampling ht = 2.5m, distance = 30 m from roadside.

The restricted data set can be examined in more detail by plotting the experimental and model results as a function of wind speed. This is shown in Figures 24 - 27 for each of the four slopes. In these Figures, results from a modified form of CALINE, denoted CALINE-\* are also presented. The modification consisted of a different formulation of the vertical dispersion coefficient as a function of the plume travel time,  $t$ , viz:

$$\sigma_z = a + b t^{0.5}$$

where  $a = 4$  m and is the wake induced vertical dispersion coefficient and  $b$  varies with atmospheric stability (2.2 for unstable, 1.1 for neutral and 0.55 for stable conditions). The value of the exponent, 0.5, has been recommended by Venkatram (1992) for modelling the dispersion of surface releases, and should be valid for distances up to about 100 m from the road. In Figure 28, the model predictions are compared to the experimental data, for a distance of 60 m from the road. It can be seen that there is reasonable agreement between the models and the measurements.

We believe, on the basis of these data that CALINE-\*, using a slope of  $1^\circ$ , performs slightly better than CALINE using a slope of  $0.5^\circ$ , however there is not much in it. If we compare CALINE-\* over the entire data set for  $\text{CO}_2$  (Figure 29), there appears to be a better correlation. Because the predicted concentrations are the product of emissions modelling and dispersion modelling, each module having an inherent uncertainty and each of which can be adjusted (for example the road slope in the former and the dispersion parameters in the latter), it is extremely doubtful whether evaluation of correlation coefficients is meaningful.

The comparisons of the predicted concentrations of CO, HC and  $\text{NO}_x$ , using a slope of  $1^\circ$ , with the experimental measurements are depicted in Figures 30 - 32 respectively. There is very good agreement for CO and  $\text{NO}_x$ , but less so for HC,



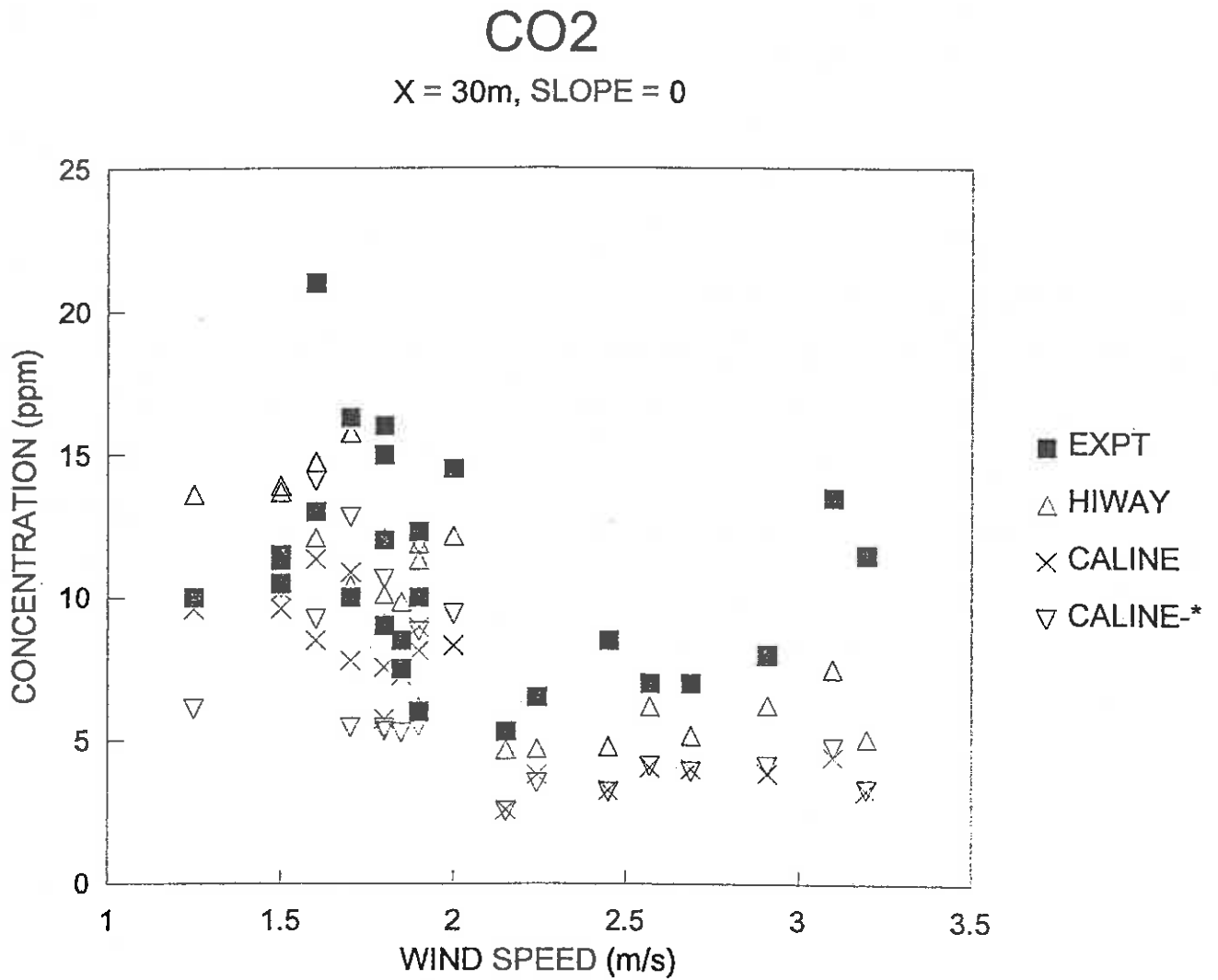


Figure 24. Comparison of predicted CO<sub>2</sub> concentrations from HIWAY, CALINE and CALINE-\* (slope=0°) with measured values as a function of wind speed: distance = 30 m from roadside.

CO<sub>2</sub>

X = 30m, SLOPE = 0.5

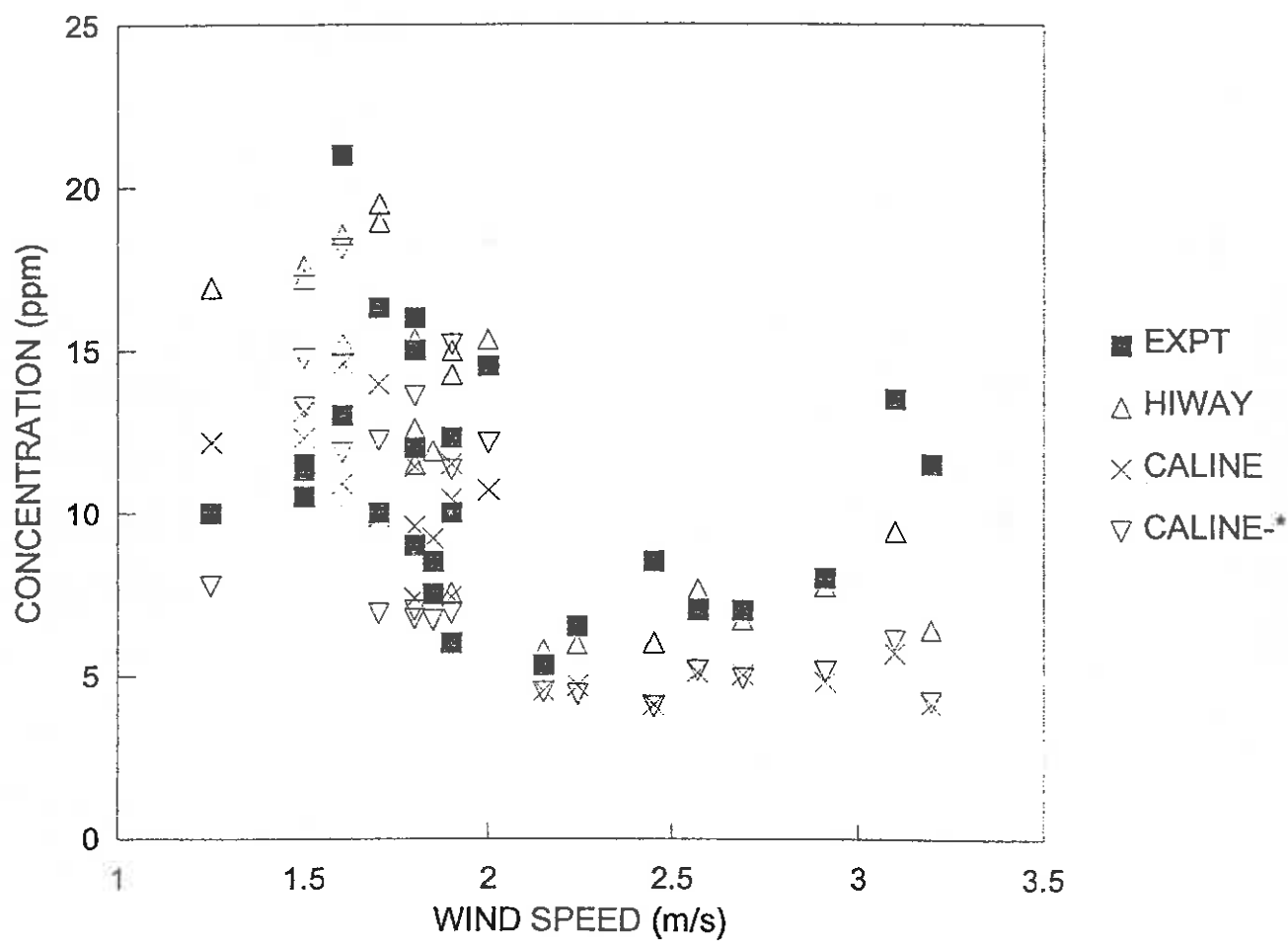


Figure 25. Comparison of predicted CO<sub>2</sub> concentrations from HIWAY, CALINE and CALINE-\* (slope=0.5°) with measured values as a function of wind speed: distance = 30 m from roadside.

CO<sub>2</sub>

X = 30m, SLOPE = 1.0

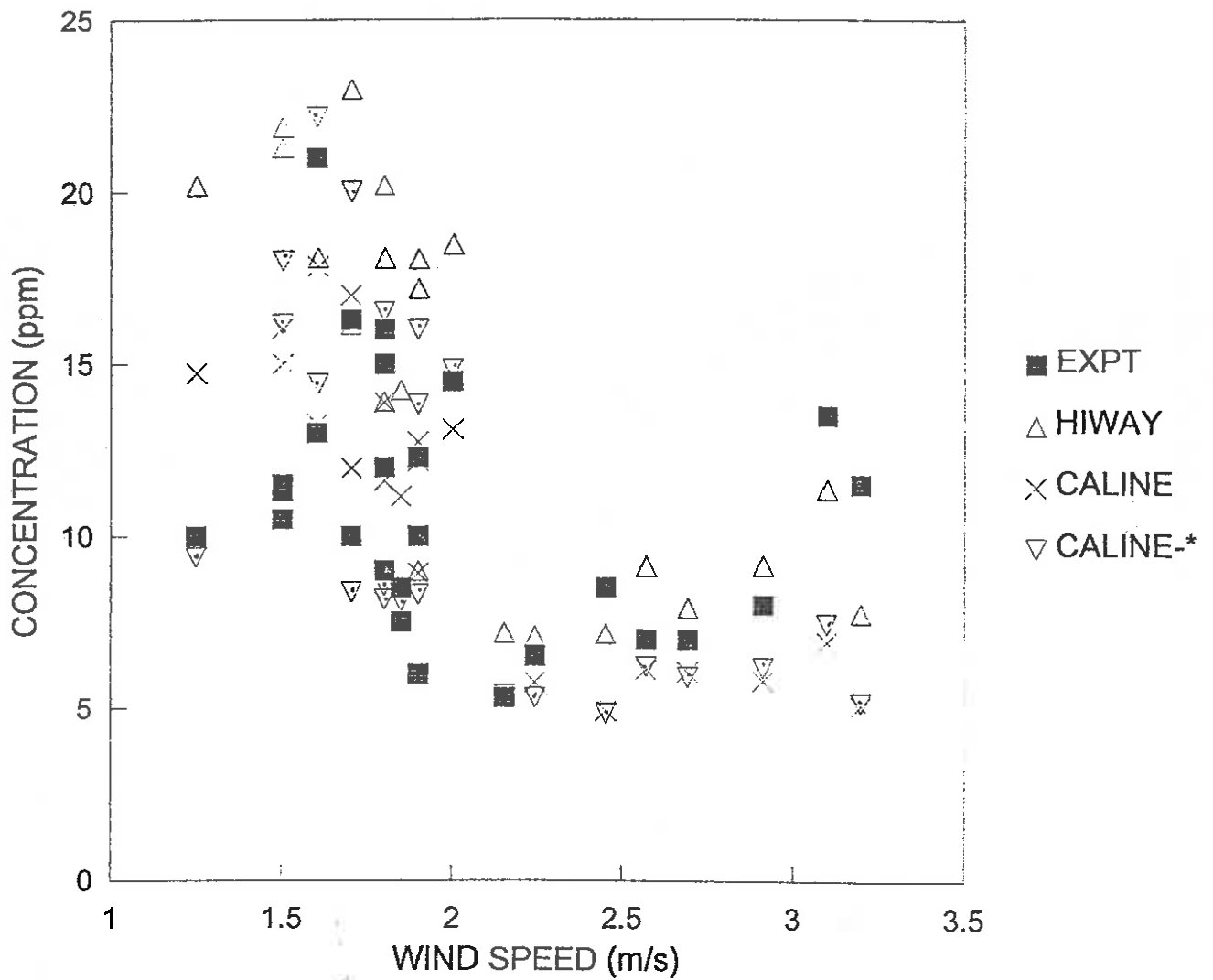


Figure 26. Comparison of predicted CO<sub>2</sub> concentrations from HIWAY, CALINE and CALINE-\* (slope=1.0<sup>0</sup>) with measured values as a function of wind speed: distance = 30 m from roadside.

CO<sub>2</sub>

X = 30m, SLOPE = 1.5

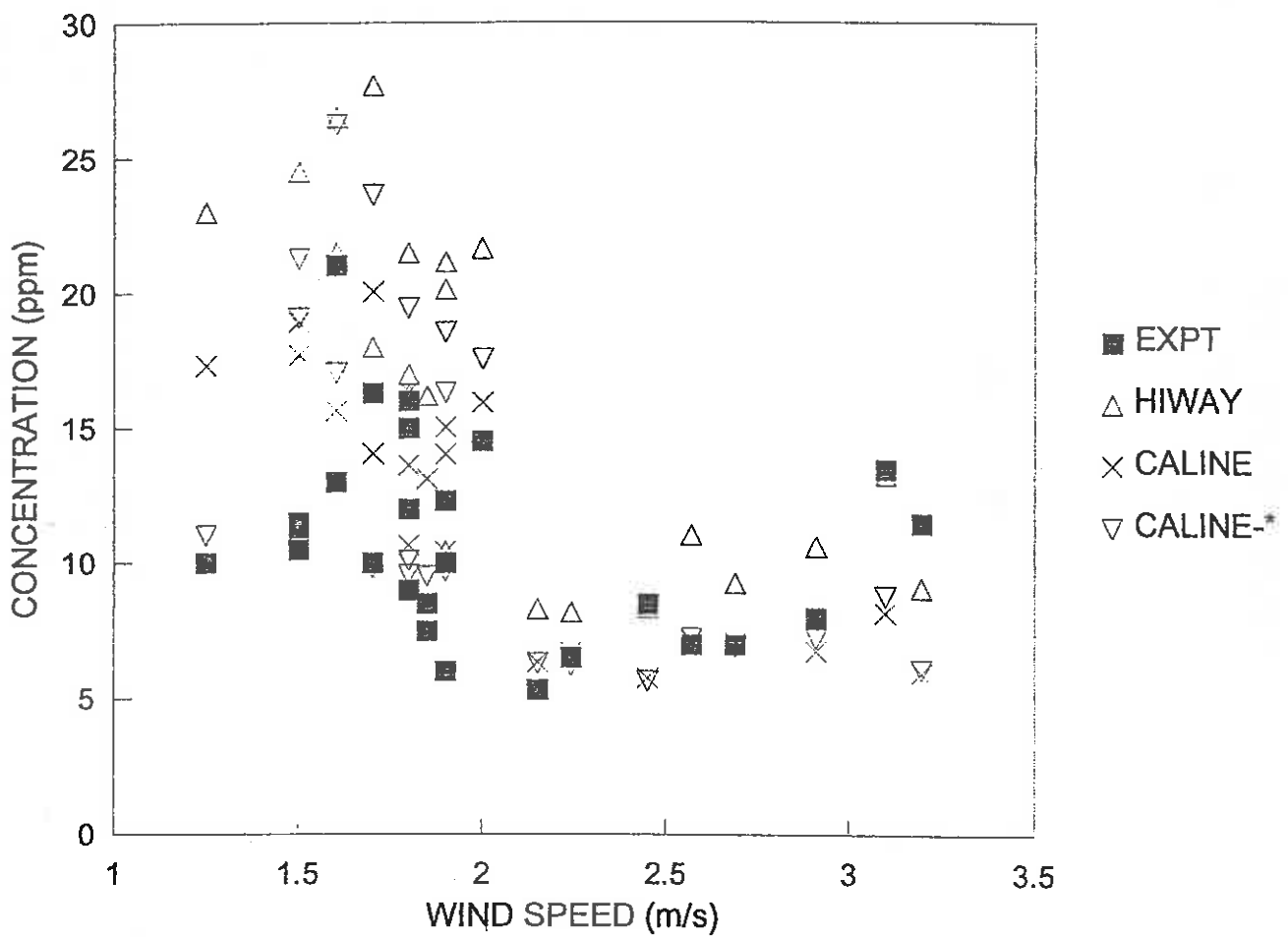


Figure 27. Comparison of predicted CO<sub>2</sub> concentrations from HIWAY, CALINE and CALINE-\* (slope=1.5°) with measured values as a function of wind speed: distance = 30 m from roadside.

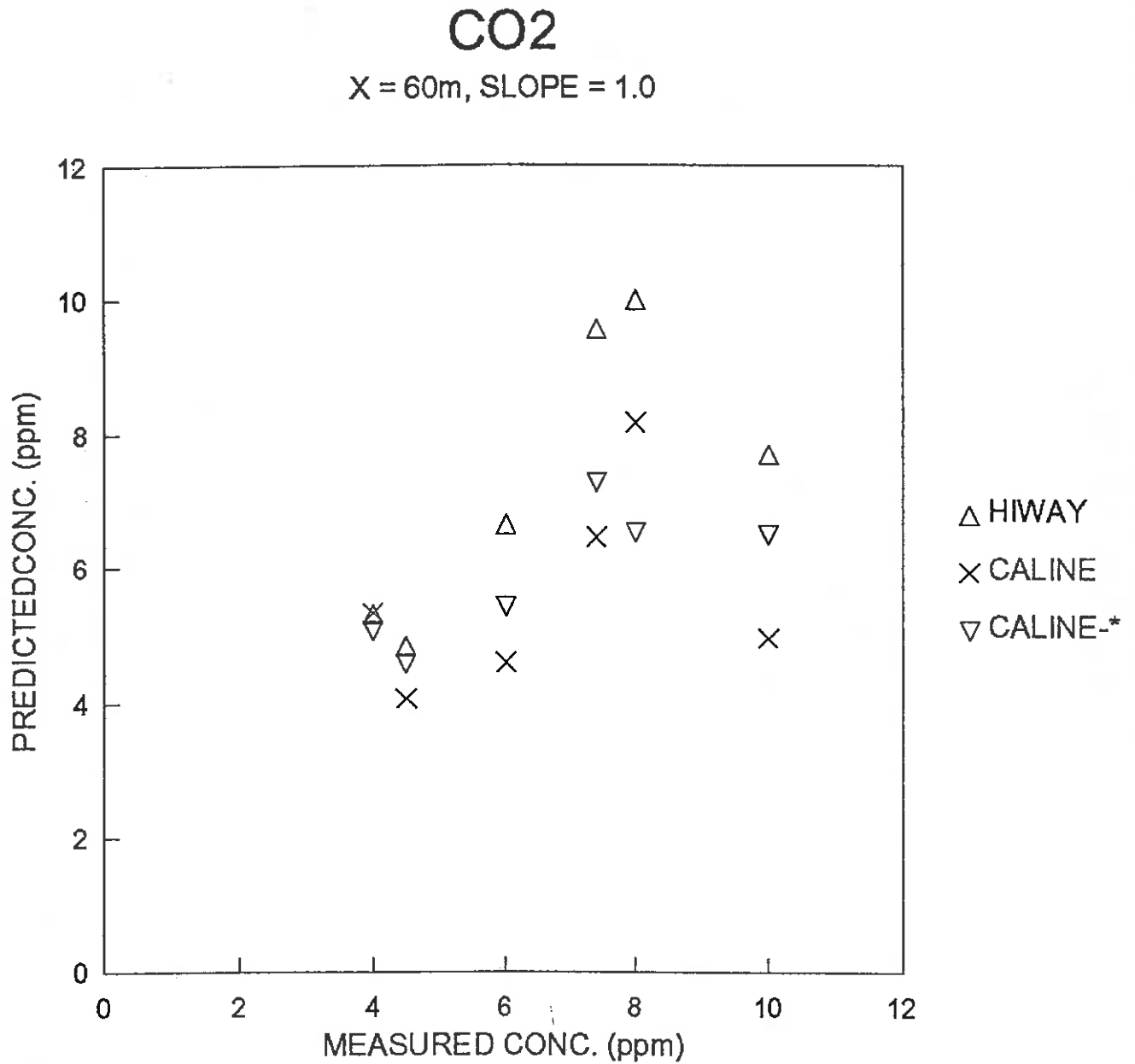


Figure 28. Predicted v measured CO<sub>2</sub> concentration for HIWAY  
CALINE and CALINE-\* : slope = 1.00  
distance = 60 m from roadside.

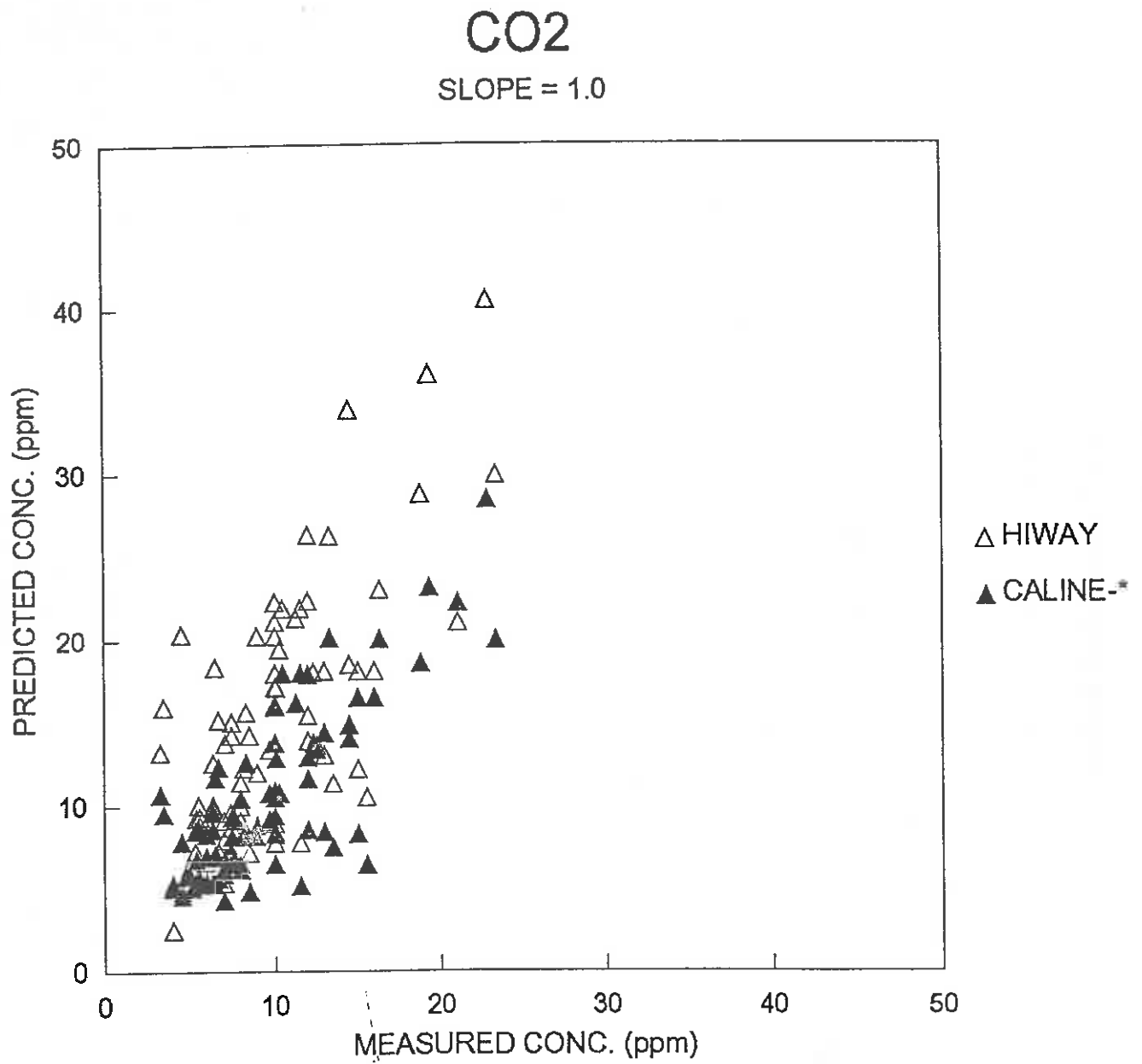


Figure 29. Predicted v measured CO<sub>2</sub> concentration for HIWAY and CALINE-\* : slope = 1.0<sup>0</sup>.

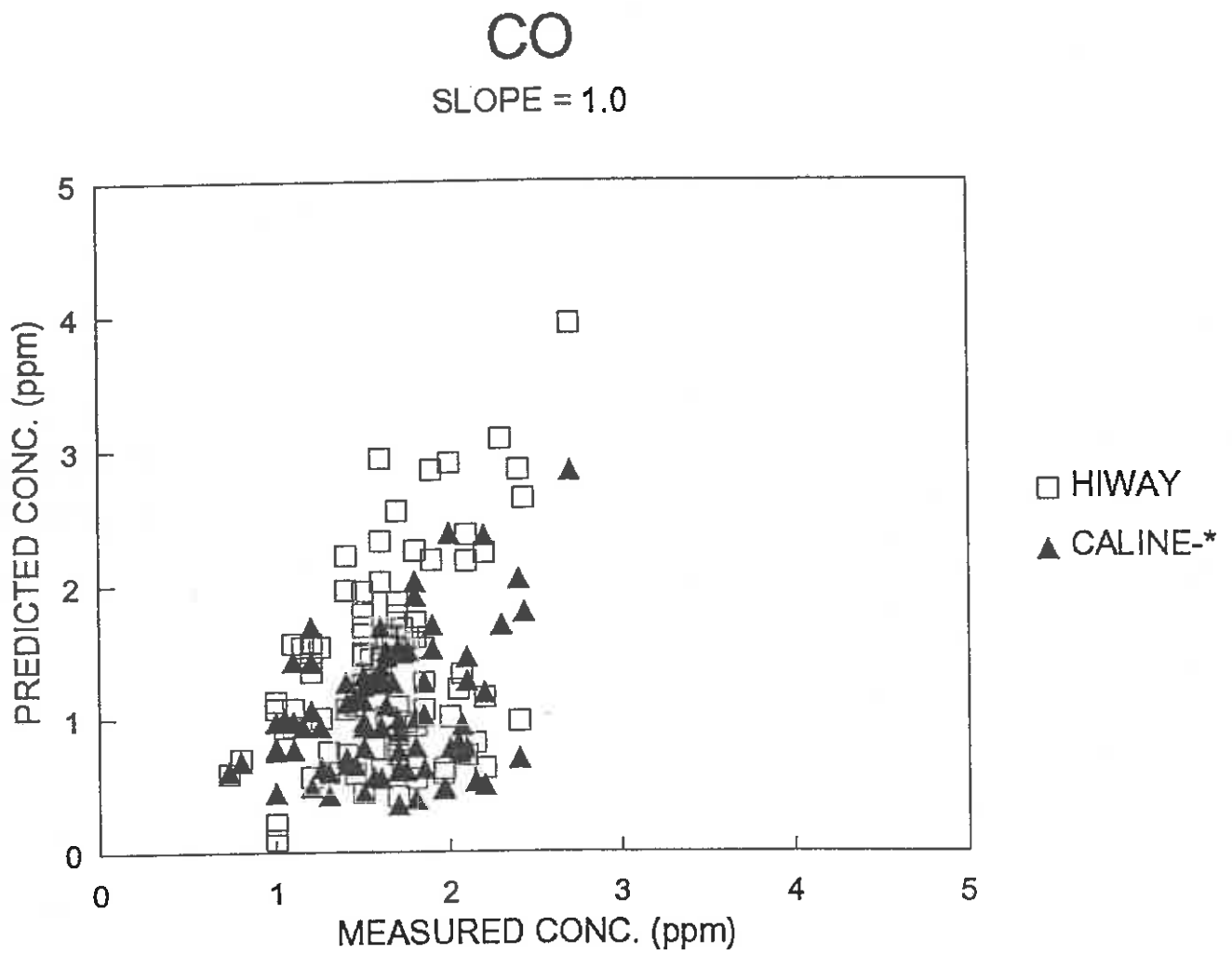


Figure 30. Predicted v measured CO concentration for HIWAY and CALINE-\* : slope = 1.00.

HC

SLOPE = 1.0

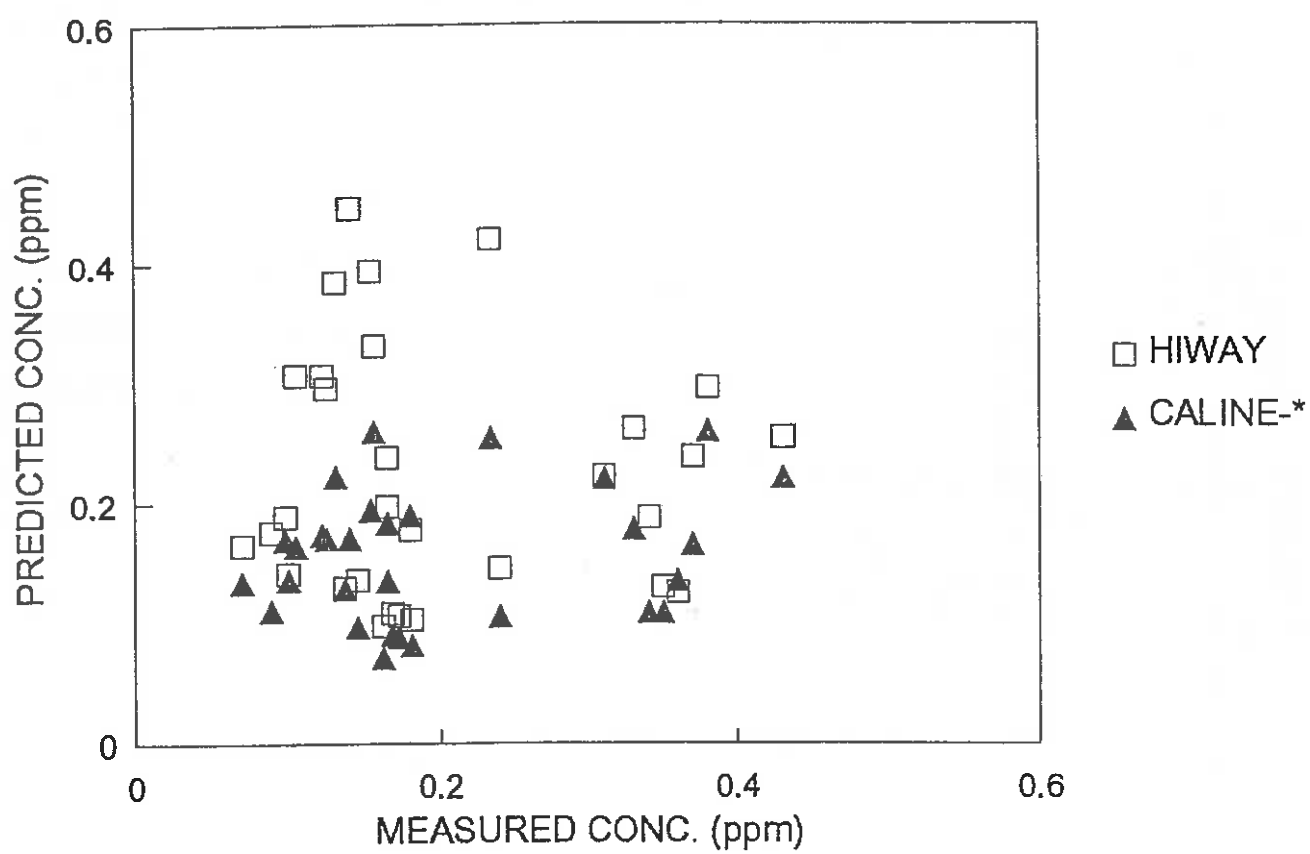


Figure 31. Predicted v measured HC concentration for HIWAY and CALINE-\* : slope = 1.00.



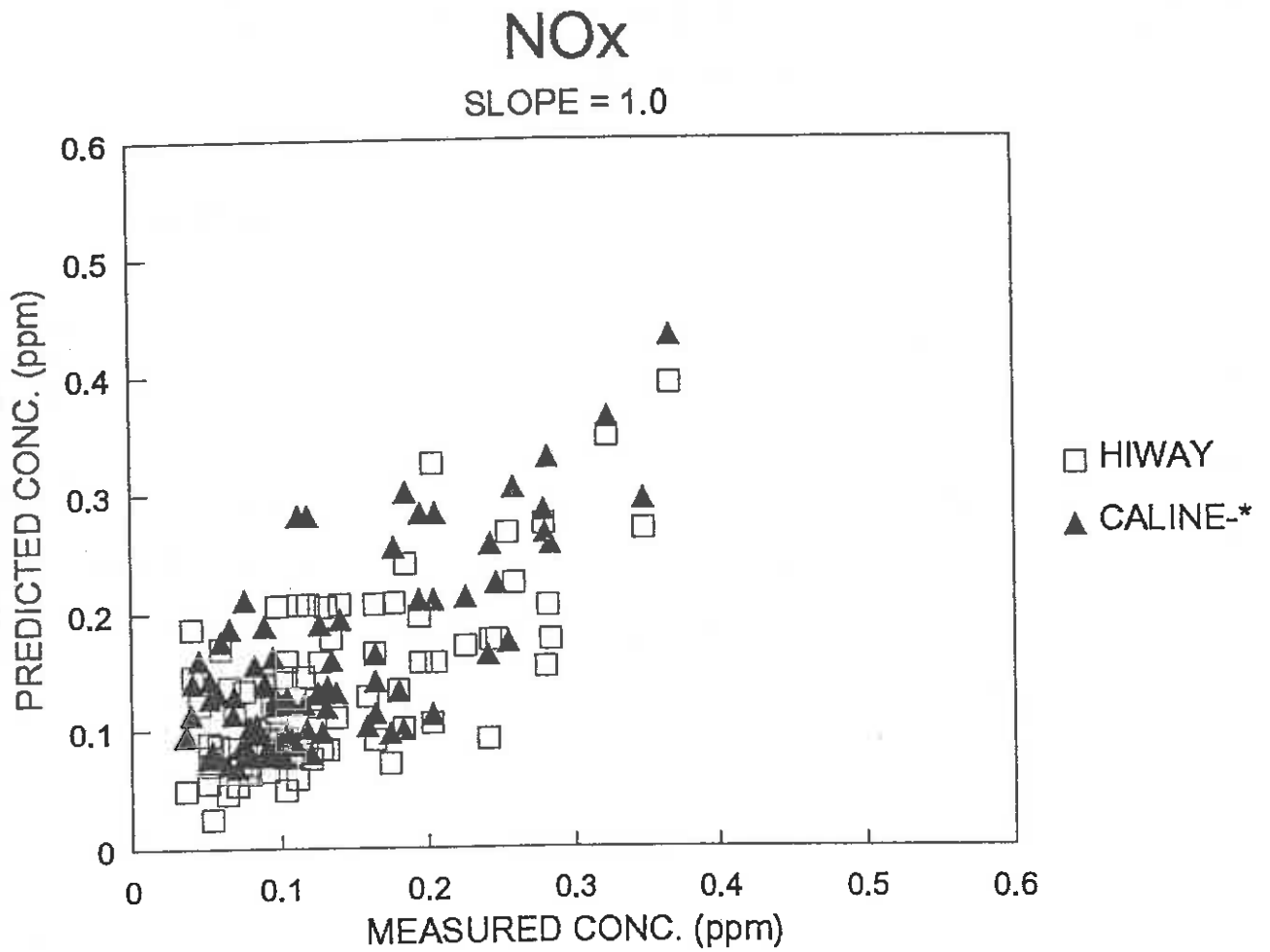


Figure 32. Predicted v measured NO<sub>x</sub> concentration for HIWAY and CALINE-\* : slope = 1.00.

which nevertheless are in the ballpark. Factors to be taken into account in respect of the HC data are that part of the HC emissions come from running losses and that background levels of HC in the ambient air are less easy to quantify and subtract from the vehicle generated HC. Also the data-set is sparser.

In estimating the input exhaust emissions, the observed traffic was only divided into heavy-duty diesels and passenger/light-duty vehicles which were lumped into the SI category, although the model can handle light-duty diesels. This is because we had no direct estimate of what proportion of light-duty commercials were in fact diesel.

Although, in practice, there is significant light-duty diesel traffic, the procedure adopted has little effect on the line emission strength. For a traffic mix of 5% heavy-duty vehicles and 5% light-duty vehicles, the CO<sub>2</sub> and NO<sub>x</sub> emission rates varied by less than 0.5% and CO and HC were reduced by 3%. These changes are insignificant within the normal scatter of the data.

A limitation of most dispersion models, certainly those used in this work, is due to the inverse dependence of concentration on the average wind speed. This means that for stalled meteorological conditions (ie  $u < 1$  m/s), which frequently occur and gives rise to the largest concentrations of pollutant, the model does not strictly apply.

Whilst the performance of the emissions module in over a drive cycle such as ADR27A provides good estimates of fuel consumption and exhaust emissions and also, in conjunction with dispersion models such as HIWAY and CALINE, good estimates of pollutant concentrations near arterial roads, there is still some fine tuning to be done, particularly in respect of deterioration factors, and on-road diesel emissions.

#### 4 RECOMMENDATIONS AND CONCLUSIONS

A power-based emission model has been developed which provides estimates of fuel consumption and the exhaust emission rates of CO<sub>2</sub>, CO, HC and NO<sub>x</sub> from spark ignition (both leaded and unleaded-fuelled) and diesel vehicles.

The model has been validated against ADR27 and ADR37 drive cycle emission data and against a Victorian methodology based on high time resolution analysis of ADR27 test results.

The emissions model, in conjunction with traffic pollution dispersion models viz: CHOCK (alias GM), HIWAY, CALINE and a slightly modified version of Caline (CALINE-\*) has been tested against field measurements of the concentrations of CO<sub>2</sub>, CO, HC and NO<sub>x</sub> made near arterial roads and shown to provide good estimates of the concentrations of these species.

Any reasonable formulated Gaussian dispersion model is likely to prove suitable for use in estimating pollutant concentrations generated by arterial roads. As CALINE (and CALINE-\*) is a more versatile dispersion model, handling, in principle, a greater range of traffic situations, it is the model of choice. Models such as CHOCK could be modified to perform satisfactorily. However, it is essential that correct emission strengths are input into such models to obtain accurate results. Stability classess B, C and D are sufficient for nearly all daytime conditions in Sydney,

Because parts of the Sydney metropolitan region are quite hilly, the utility of emission models based on drive cycle emission data with various adjustment factors is questionable. It is recommended that a more physically based-model, capable of incorporating slopes and other accelerations is used in such circumstances.

## 5 REFERENCES

- Cadle S.H., Gorse R.A. and Lawson D.R. 1993. Real-world vehicle emissions - a summary of the third annual CRC-APRAC on-road vehicle emissions workshop. *Air and Waste*, 43, 1084-1090.
- Carnovale F., Alviano P., Carvalho C., Deitch G., Jiang S., Macaulay D. and Summers M. 1991. Air emissions inventory Port Phillip Control Region. Report of the EPA(Vic) SRS 91/001.
- Chock, D.P. 1978. A simple line-source model for dispersion near roadways. *Atmos. Environ.* 12. 823-829.
- Draxler R.R. 1976. Determination of atmospheric diffusion parameters. *Atmos. Environment*, 10, 99-105
- Guensler R., Washington S., Koenig B. and Sperling D. 1993. The impact of speed correction factor uncertainty on mobile source emission inventories in the South Coast. *Proc. Int. Speciality Conf. "The Emission Inventory - Perception and Reality"*, Pasadena, California, Oct. 18-20. Air and Waste Management Assoc.
- Kent, J.H. and Mudford, N.R. 1978. Sydney driving patterns and automotive emission modelling. Charles Kolling Research Lab., UNSW Tech. Rep. ER-26.
- Kent, J.H., K. Post, J.A. Tomlin. 1982. Second Conference on Traffic, Energy and Emissions, 19-20 May 1982 at the National Science Centre, Melbourne.
- Post, K., J.A. Tomlin, D. Pitt, N. Carruthers, A. Maunder, T. Gibson, J.H. Kent and R.W. Bilger. 1981. Fuel Consumption and Emissions Research Annual Report by

the University of Sydney for 1980-81 Charles Kolling Research Laboratory Technical Note ER 36.

Rao, S.T. and M.T. Keenan. 1980: Suggestions for improvement of the EPA-HIWAY model. JAPCA 30: 247-256.

Richardson A.J. 1982. Stop-start fuel consumption rates. Second Conference on Traffic, Energy and Emissions, 19-20 May 1982 at the National Science Centre, Melbourne.

Robinson N.F., Pierson W.R. and Gerler A.W. 1993 Comparison of real world CO, VOC and NO<sub>x</sub> emission rates with motor vehicle emission models. Proc. Int. Speciality Conf. "The Emission Inventory - Perception and Reality", Pasadena, California, Oct. 18-20. Air and Waste Management Assoc.

SPCC 1989. Annual Report 1988/89. State Pollution Control Commission of New South Wales.

Venkatram A. 1992. Vertical dispersion of ground-level releases in the surface boundary layer. Atmos. Environment, 26A, 947-949.

Williams, D.J., Milne, J.W., Roberts, D.B. and Kimberlee, M.C. 1989. Particle emissions from 'in-use' motor vehicles - I. Spark ignition vehicles. Atmos. Environment, 23, 2639-2646.

Williams, D.J., Milne, J.W., Quigley, S.M., Roberts, D.B. and Kimberlee, M.C. 1989. Particle emissions from 'in-use' motor vehicles - II. Diesel vehicles. Atmos. Env. 2647-2662.

Williams D.J., Carras J.N., Drummond M.S., Lange A.L. and Shenouda D.A. 1993.  
Interim Report to the RTA on air pollution near arterial roads and highways.  
Investigation Report CET/IR184.